

**INVESTIGATION OF TUMOR CELL INTRINSIC AND EXTRINSIC
REGULATORS OF PANCREATIC NEUROENDOCRINE
TUMORIGENESIS**

by

Karen Elizabeth Hunter

A Dissertation

Presented to the Faculty of the Louis V. Gerstner, Jr.

Graduate School of Biomedical Sciences,

Memorial Sloan-Kettering Cancer Center

in Partial Fulfillment of the Requirements for the Degree of

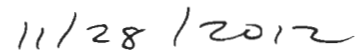
Doctor of Philosophy

New York, NY

November, 2012



Johanna A. Joyce, PhD
Dissertation Mentor



Date

Copyright by Karen E. Hunter 2012

DEDICATION

To my parents, for all of their love and support.

ABSTRACT

Pancreatic neuroendocrine tumors (PanNETs) are a relatively rare, but clinically challenging tumor type, due to their marked disease heterogeneity and limited understanding of the molecular basis for their development. The objective of my thesis research is to identify tumor cell intrinsic and extrinsic regulators of PNET pathogenesis using patient samples in combination with the RT2 mouse model of insulinoma.

Heparanase is a matrix-remodeling enzyme, which cleaves heparan sulfate side chains within heparan sulfate proteoglycans, an abundant component of the extracellular matrix. Using tumor tissue microarrays obtained from patients with well-differentiated PanNETs we have found that heparanase expression is significantly correlated with increased malignancy and metastasis in patients with PanNETs. To elucidate the mechanisms by which heparanase promotes pancreatic neuroendocrine tumors we utilized the RIP1-Tag2 (RT2) transgenic mouse model crossed to transgenic mice that constitutively overexpress human heparanase (*Hpa-Tg*) or heparanase knockout RT2 mice to examine the effects of genetically modulating heparanase levels *in vivo*.

Our analysis revealed that heparanase promotes tumor invasion, and that this invasion is both tumor cell- and macrophage-derived. Further characterization of *Hpa-Tg* RT2 mice revealed a significant increase in peritumoral lymphangiogenesis *in vivo* and that *Hpa-Tg* macrophages have an increased

ability to form lymphatic endothelial-like structures in cell culture. Conversely, we found that heparanase knock-out led to increased angiogenesis and pericyte coverage. Together, these data describe multiple novel roles for heparanase in promoting PanNET tumorigenesis.

In addition, we have identified a previously undescribed subset of RT2 tumors that were negative for multiple β -cell islet markers, highly invasive and anaplastic that we termed poorly differentiated invasive carcinomas (PDIC). These tumors exhibited a high proliferation index, similar to high-grade poorly differentiated PanNETs (PD-PanNET). Interestingly, we have identified Id1 as being specifically expressed in PDICs. We have established the tools to investigate the development and molecular mechanisms driving this tumor type *in vivo*. In parallel, we have initiated the development of a mouse model for PD-PanNETs for use in preclinical testing, as none currently exists.

BIOGRAPHICAL SKETCH

Karen Elizabeth Hunter was born and raised in Drumore, Pennsylvania. From kindergarten through high school she attended the public schools of Solanco School District. Her interest in science was sparked by her high school AP Chemistry teacher, Mr. Griffiths, and her AP Biology teacher, Mr. Miller. She then moved to Cambridge, Massachusetts to study Biological-Chemical Engineering (Course 10B) at the Massachusetts Institute of Technology. During the course of her studies at MIT, she developed a strong interest in molecular biology, taking enough electives to earn an additional major in Biology.

During her undergraduate years, Karen was involved with research in many fields spanning biology and bioengineering. She spent one summer studying neutrophil adhesion in Dr. Scott Simon's lab at the University of California, Davis, and another summer studying the Nogo receptor in nerve generation in the Neurobiology Research division of Biogen Idec. Karen also spent time in Dr. Dane Wittrup's laboratory at MIT, assisting a graduate student in developing pretargeted radioimmunotherapies. In addition, she was a research assistant in Dr. David Sweetser's laboratory at Massachusetts General Hospital, studying the role of TLE1 and TLE4 in leukemia. Upon graduating from MIT in 2006, Karen was a Howard Hughes Medical Institute research technician in the laboratory of Dr. Angelika at the Center for Cancer Research at MIT, studying the effects of aneuploidy on mammalian cells. During her time working at MIT, she gained

exposure to the power of mouse models to study cancer development and decided to pursue a PhD focusing on cancer biology.

Karen chose to pursue her graduate studies in Cancer Biology at the Gerstner Sloan-Kettering Graduate School of Biomedical Sciences because of its focus on the integration of the basic science and clinical aspects of cancer research. She joined the laboratory of Dr. Johanna Joyce in 2008 to study the tumor microenvironment for her graduate research. Karen was awarded a National Science Foundation honorable mention and a Grayer Fellowship.

ACKNOWLEDGEMENTS

First and foremost I would like to thank my outstanding thesis advisor, Dr. Johanna Joyce. I have been inspired by her passion for science and for her lab members, and I am extremely fortunate to have had the opportunity to be part of such a great group. Her mentorship has taught me so much about how to think critically about science and how to communicate about scientific matters. I truly appreciate my experience in the Joyce lab and cannot thank her enough.

I would also like to thank my thesis committee members, Dr. Andrew Koff and Dr. Jacqueline Bromberg, who have provided support and important insights into my research throughout my graduate studies. In addition, I would like to thank Dr. David Solit for serving as my thesis defense chairperson.

The members of the Joyce lab have created an intellectually stimulating, fun, and supportive environment over the years. I would like to particularly acknowledge Carmela Palermo for initiating the heparanase project, and Karoline Dubin and Jemila Kester for their assistance. I've been fortunate to work with many great lab members, including Leila Akkari, Bobby Bowman, Tina Elie, Bedrick Gadea, Leny Gocheva, Alberto Jimenez-Schuhmacher, Steve Mason, Oakley Olson, Stephanie Pyonteck, Daniela Quail, Lisa Sevenich, Tanaya Shree, Hao-Wei Wang, and Dongyao Yan. I have also been significantly aided by the fantastic technical and administrative support of Xiaoping Chen, Julissa Nunez, Ben Prewitt, and Kenishana Simpson.

I am grateful for the support from our collaborators, in particular Dr. Israel Vlodavsky and Dr. Robert Benezra, for mice that were invaluable for my research. I would also like to thank Dr. Laura Tang for patient samples and Dr. Diane Reidy-Lagunes for important discussions on PanNETs. My research on these projects was funded in part by a Cycle for Survival grant; Cycle for Survival grants provide important resources for researching underfunded rare cancers. I also would like to thank everyone in the GSK Graduate School for creating an excellent graduate program and working tirelessly to provide the best graduate experience possible.

Lastly, I would like to thank my family and friends for their continued support. My father and brother have been supportive of everything that I've done. My mother, Sally Hunter, has always encouraged me to strive for more, and provided me with the many opportunities that have allowed me to achieve what I have today. I cannot thank her enough. I also am thankful for my boyfriend, Kevin Cohn, who has been a steadfast supporter of me throughout my research and dissertation.

TABLE OF CONTENTS

CHAPTER ONE.....	1
Introduction	1
PanNETs.....	2
RIP1-Tag2 model of PanNETs	6
Importance of the tumor microenvironment	9
Cancer inflammation	11
Tumor lymphangiogenesis.....	12
Remodeling of the ECM during tumorigenesis	15
Heparan sulfate.....	15
Heparanase cleaves HSPGs	16
Heparanase in tumor progression and metastasis	19
Thesis aims	21
CHAPTER TWO.....	23
Materials and Methods	23
Transgenic mice	23
Bone marrow transplantation (BMT) protocol	23
Tissue processing and analysis	24
Immunohistochemistry (IHC) and immunofluorescence (IF) staining	24
IHC and IF tissue analysis.....	26
Assay for trans-differentiation of BMDM into LEC-like structures	26
Flow cytometry and sorting	27
RNA isolation and qRT-PCR	28
Western blotting	29
Tumor cell line infections.....	29
Human PanNET samples.....	29

Statistical analysis	30
CHAPTER THREE	32
Heparanase Promotes Tumorigenesis in PanNETs	32
Results	33
Heparanase expression is associated with malignant progression in human pancreatic neuroendocrine tumors	33
Genetic manipulation of heparanase levels in the RIP1-Tag2 PanNET model	37
Heparanase promotes pancreatic neuroendocrine tumor invasion	39
Macrophage supplied heparanase promotes tumor invasion	43
Cancer cell- and TAM-supplied heparanase promote tumor invasion	45
Heparanase deletion leads to increased tumor angiogenesis	50
Heparanase overexpression enhances peritumoral lymphangiogenesis.....	53
Growth factor expression is not affected by heparanase modulation	55
Heparanase overexpression enhances formation of LEC-like structures	58
Discussion	64
Heparanase expression promotes tumorigenesis in PanNETs	64
Heparanase promotes invasion through cancer cell and TAM sources.....	65
Heparanase plays pleiotropic roles in the tumor microenvironment	68
CHAPTER FOUR	72
Characterization and Development of a Mouse Model of Poorly Differentiated PanNETs	72
Results	73
Identification of a novel class of invasive, poorly differentiated tumors	73
PDICs exhibit a high mitotic index	73
PDICs occur in the majority of RT2 mice	76
PDICs exhibit loss of neuroendocrine markers.....	77
PDICs specifically express Id1	80

Development of mouse models to study PD-PanNETs	86
Discussion	88
Identification of PDICs in RT2 mice	88
How do PDICs develop?	91
Development of a mouse model of PD-PanNETs.....	94
CHAPTER FIVE	95
Conclusions, Perspectives and Clinical Implications	95
Conclusions.....	95
Heparanase promotes PanNET tumorigenesis	95
Characterization and development of a mouse model of PD-PanNETs	96
Perspectives and Clinical Implications	97
The multifaceted role of heparanase in tumorigenesis	97
Complexities of targeted ECM remodeling enzymes	99
Heparanase as a therapeutic target.....	99
Origin of PDICs	101
Development of a mouse model of PD-PanNETs.....	102
BIBLIOGRAPHY	104

CHAPTER ONE

Introduction

Cancer remains a major public health problem in the United States and around the world, with one in four deaths in the U.S. due to cancer (Siegel et al., 2012). In 2012 it is expected that there will be over 1.6 million new cases of cancer diagnosed in the U.S. alone. Rare cancers, such as pancreatic neuroendocrine tumors (PanNETs), are described as those with a prevalence of less than 200,000 patients in the U.S., and research into these tumor types has been lagging. However, half of all cancer diagnoses are considered rare, underlining the urgent need to characterize and understand these rare tumor types.

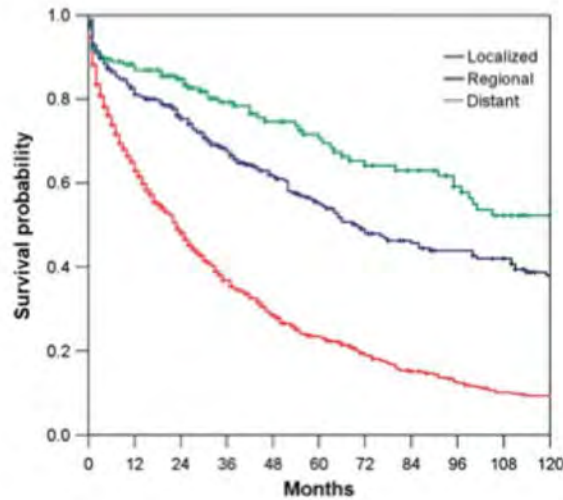
The objective of my thesis research is to further our understanding of PanNETs by identifying tumor cell intrinsic and extrinsic regulators of PanNET pathogenesis using patient samples in combination with the RIP1-Tag2 mouse model of insulinoma. My focus on tumor cell extrinsic regulators has primarily investigated the role of the matrix remodeling enzyme heparanase, and its roles in promoting processes including tumor invasion and lymphangiogenesis. In addition, my thesis research has identified a novel class of poorly differentiated tumors that I have characterized and which are being used to develop a mouse model of poorly differentiated PanNETs.

PanNETs

Pancreatic neuroendocrine tumors (PanNETs) are a rare but clinically challenging tumor type; a consequence of marked disease heterogeneity and limited understanding of the molecular basis for these cancers, among other factors. PanNETs arise from cells of the neuroendocrine system within the pancreas and include insulinomas, gastrinomas, glucagonomas, VIPomas and somatostatinomas (Davies and Conlon, 2009). Well-differentiated, low to medium grade PanNETs can be classified into two groups: functional tumors that secrete hormone, which represent 30% of patients, and nonfunctional tumors which do not secrete hormone (Reidy-Lagunes, 2012). Well-differentiated PanNETs are clinically distinct from poorly differentiated, high-grade PanNETs (PD-PanNETs) which are characterized by a high mitotic index (Reidy et al., 2009).

PanNETs are the second most common pancreatic neoplasms, representing approximately 1.3% of pancreatic cancers in incidence and 10% of cases in prevalence (Yao et al., 2007). PanNETs have diverse clinical outcomes, in which some patients can exhibit long-term survival, although the overall 10-year survival rate is only 40%. PanNET patients often present with local lymph node metastasis and in addition, PanNETs show a remarkable tropism for the liver (Reidy et al., 2009). Those patients with distant metastatic dissemination have a median survival of only 24 months (Figure 1.1A) (Yao et al., 2007). PanNETs patients with nonfunctioning tumors make up a disproportionate number of

A



B

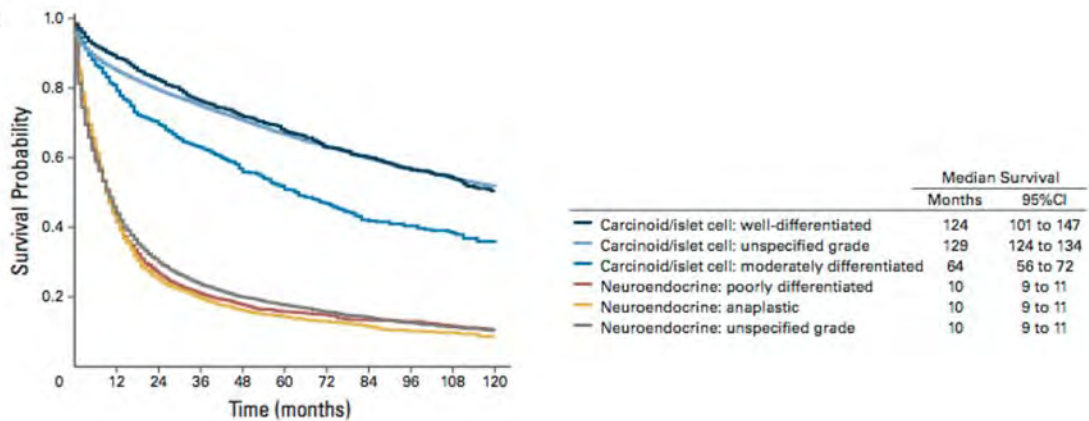


Figure 1.1. Survival statistics for PanNET patients. (A) Stage and survival of 1157 patients from the time of diagnosis. Median duration of survival of patients with localized ($n = 167$), regional ($n = 289$), and distant disease ($n = 558$) was 124, 70, and 23 months, respectively ($P < 0.001$). (From Yao, et al., 2007) (B) Survival duration by histology. Median survival durations are presented in months (with 95% confidence intervals (CIs)). (From Yao, et al., 2008).

patients with poor prognosis, as they grow silently and present with extensive metastatic disease at diagnosis. Patients with PD-PanNETs represent the worst prognosis of the entire PanNET spectrum (Figure 1.1B) (Yao et al., 2008).

It is currently unknown whether nonfunctioning tumors arise from a different cell of origin to hormone-producing neoplasms or reflect a more stem-like differentiation status. It has been hypothesized that they originate from pluripotent cells in the ductal epithelium, which maintain their ability to differentiate toward the various hormone-producing neoplasms (Davies and Conlon, 2009). Also, while it is thought that well-differentiated PanNETs arise from the various neuroendocrine cells of the pancreas, the cell of origin for PD-PanNETs is controversial. It has been proposed that PD-PanNETs may arise from a separate, potentially non-neuroendocrine lineage (Reidy et al., 2009). However, as patients often present with advanced disease, the disease course of PanNETs is obscure.

A recent study by the Vogelstein group investigated the genomic landscape of PanNETs, in which whole exome sequencing was performed on 10 well-differentiated PanNET samples, with further sequencing for selected genes on an expanded cohort of 58 patients. Mutations in chromatin remodeling gene subunits (DAXX/ATRX) were identified in 43% of patients examined, and MEN1 tumor suppressor mutations in 44% of patients (Jiao et al., 2011). These mutations (DAXX/ATRX and MEN1) were found to correlate with better patient

prognosis, potentially identifying a new subclass of PNETs; however genes that are positively associated with poor prognosis critically still remain elusive.

Patients with PanNETs are treated with surgical resection, liver-directed therapies and systemic therapies. Surgical resection is the most effective treatment option for PanNETs; however, approximately 65% of patients present with unresectable or metastatic disease. Conventional chemotherapy does not have a clearly defined role in this tumor type, with highly variable response rates and no standard regimens (Reidy-Lagunes, 2012). Somatostatin analogs (e.g. octreotide) are highly useful for the treatment of hormone-producing PanNETs, due to their anti-proliferative effects, however many patients do not express somatostatin receptors and thus are not receptive to this therapy (Reidy-Lagunes, 2012). Two targeted therapies, everolimus and sunitinib malate, were approved by the U.S. Food and Drug Administration (FDA) in 2011, the first new drug approvals for this tumor type in 30 years (Vogelzang et al., 2012). Everolimus, an mTOR inhibitor, significantly increased progression-free survival (11.0 vs. 4.6 months) (Yao et al., 2011) as did sunitinib malate, a VEGFR and PDGFR inhibitor (11.4 vs. 5.5 months) (Raymond et al., 2011). However, even though these newly approved drugs improve progression-free survival, the objective RECIST-defined tumor response rates are still relatively low, no significant benefits in overall survival have been shown, and these drugs are associated with nontrivial toxicities (Kulke et al., 2011), indicating the continued need for novel therapies in PanNETs.

PD-PanNETs respond very differently to therapeutic agents than well-differentiated PanNETs and thus are treated with a different regimen. These tumors are generally managed with surgery and platinum-based chemotherapy (Moertel et al., 1991). Unfortunately, little is currently known about how to stratify patients based on their prognosis, nor the use of targeted therapies for PD-PNETs with unresectable metastases.

RIP1-Tag2 model of PanNETs

As effective, non-surgical therapies for PanNETs have been limited, the RIP1-Tag2 (RT2) mouse model of islet-cell carcinoma has proven very informative in studying neuroendocrine tumor progression, and in particular, in predicting clinical efficacy of new therapeutics (Tuveson and Hanahan, 2011). In this model, β -cell specific expression of the SV40 T-antigen leads to islet-cell carcinomas through a reproducible and well-characterized tumor progression pathway (Figure 1.2) (Hanahan, 1985). At 4-6 weeks of age, approximately 50% of the approximately 400 islets in the pancreas begin to proliferate rapidly and are called hyperplastic islets (Ribatti et al., 2007). A quarter of these proliferative islets acquire the ability to induce their normally quiescent vasculature to undergo angiogenic switching and are termed angiogenic islets (Folkman et al., 1989). Approximately 15-20% of these angiogenic islets progress to form tumors, resulting in 10-15 tumors per mouse. The tumors that develop resemble human PanNETs histologically and express high levels of insulin, which causes the mice to succumb to hypoglycemia by 13-17 weeks of age. The tumors that develop

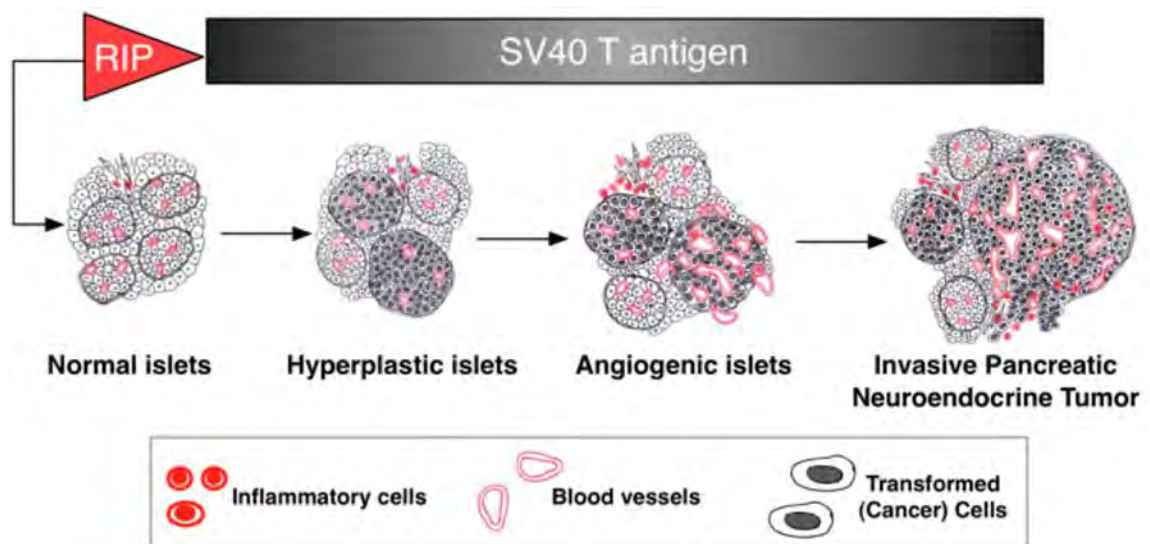


Figure 1.2. The RIP1-Tag2 transgenic mouse model of pancreatic neuroendocrine tumorigenesis. Adapted from Reinheckel T, Gocheva V, Peters C and Joyce JA (2008). Roles of cysteine proteases in tumor progression: analysis of cysteine cathepsin knockout mice in cancer models. In “The Cancer Degradome”, D Edwards, G Hoyer-Hansen, F Blasi and BF Sloane, eds, Springer.

exhibit a spectrum of tumor invasion that can be scored histologically into three categories: (1) encapsulated tumor (Tum) in which the tumor is well-defined by a collagen capsule and with no invasion; microinvasive carcinoma (IC1) in which focal invasion has occurred; and invasive carcinoma (IC2) in which widespread invasion has occurred on multiple fronts (Lopez and Hanahan, 2002). The RT2 model also mimics human PanNETs as pancreatic islet cell tumors metastasize with low frequency to both the intra-pancreatic lymph nodes and the liver (Paez-Ribes et al., 2009).

While this mouse model utilizes a viral oncogene, SV40 T-antigen, to inactivate the p53 pathway and induce tumorigenesis in pancreatic islet cells, which is not the mechanism of tumor initiation in humans, a recent study has shown that negative regulators of the p53 pathway are aberrantly activated in approximately 70% of PanNETs (Hu et al., 2010). Increased levels of these negative regulator proteins, MDM2, MDM4 and WIP1, thus leads indirectly to a decrease in p53 activity (Hu et al., 2010). Therefore, the RT2 model targets the same pathways as genetic alterations observed in a majority of PanNETs.

Many studies have investigated the molecular mechanisms of tumor progression in the RT2 model, which have provided important insights into multistage tumorigenesis and, in particular, islet cell carcinogenesis. Extensive macrophage infiltration is observed during RT2 tumorigenesis, particularly in invasive tumors (Gocheva et al., 2010), and analysis of macrophage density in patient PanNET

samples revealed a highly significant, positive correlation with poor patient prognosis and metastasis (Pyonteck et al., 2012). Importantly, the RT2 model has been shown to have critical predictive value for clinical studies, predicting response to the recently FDA-approved drugs sunitinib malate and everolimus (Chiu et al., 2010; Paez-Ribes et al., 2009; Raymond et al., 2011; Yao et al., 2011).

Importance of the tumor microenvironment

Tumors develop in a complex microenvironment comprising cancer cells surrounded by a diverse set of stromal cells including fibroblasts, blood and lymphatic endothelial cells, and a variety of bone-marrow derived cells (Figure 1.3) (Joyce and Pollard, 2009). The importance of the tumor microenvironment was first described in Paget's "seed and soil" hypothesis, in which he proposed that metastatic spread was not simply random, but was profoundly influenced by the "soil" in which metastatic tumor "seeds" landed (Paget, 1989). In another seminal body of work, Dr. Judah Folkman proposed that tumors were dependent on angiogenesis, suggesting that targeting the endothelial cells and the vasculature within tumors would inhibit tumor growth (Folkman, 1971). Indeed, his hypothesis initiated an entire field of angiogenesis research and led to the development of anti-angiogenic therapies, such as sunitinib malate used in the clinic today. The tumor microenvironment has since been established as playing a critical role in tumorigenesis and response to therapy through the secretion of

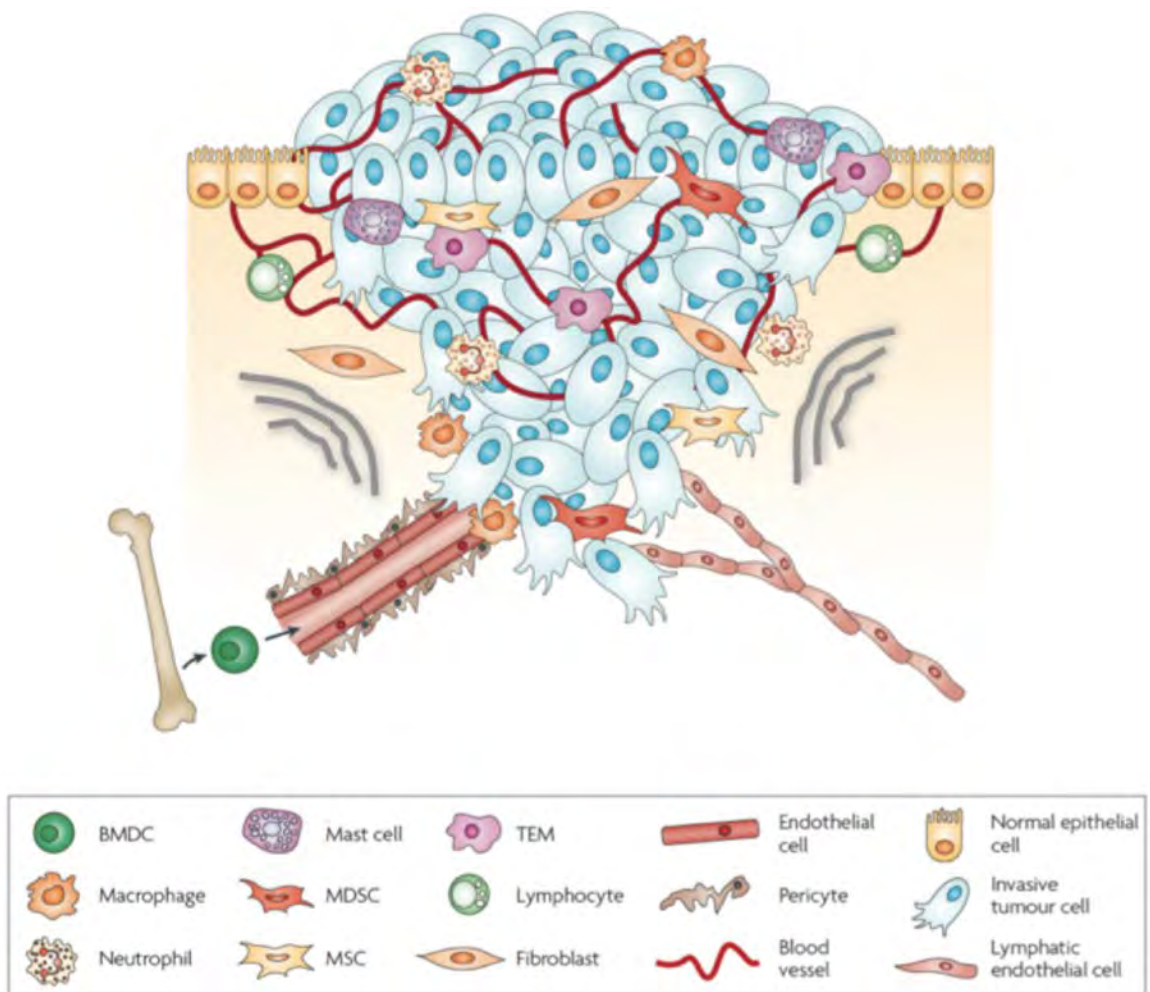


Figure 1.3. The complex tumor microenvironment. Solid tumor microenvironments are composed not only of tumor cells, but also of many types of stromal cells, including cells that compromise the vasculature and lymphatics, cells of the immune system, as well as other connective tissue cell types. Non-cellular components such as the extracellular matrix (grey lines) can also have a profound impact on tumor biology. *Adapted from Joyce & Pollard (2009).*

growth factors, chemokines, cytokines and proteases and remodeling of extracellular matrix (Joyce and Pollard, 2009).

Cancer inflammation

In 1863, the pathologist Rudolf Virchow, referred to as the “father of modern pathology” made one of his many seminal observations, that tumors frequently contain a substantial immune cell infiltrate. While it was initially thought that these cells were a failed attempt to attack the tumor, it is now accepted that immune cells and the inflammatory environment associated with them can play critical roles in promoting tumorigenesis (Joyce and Pollard, 2009). Indeed, chronic inflammation establishes a pro-tumorigenic microenvironment and has been linked to 15-20% of all deaths from cancer worldwide (Mantovani et al., 2008). Cancer-related inflammation has been shown to promote cell proliferation, survival and the epithelial-mesenchymal transition, and to induce angiogenesis and lymphangiogenesis. In addition, inflammatory cells can promote tumor cell invasion and metastasis, inhibit adaptive immunity, and alter response to therapy (Mantovani et al., 2008).

One of the key and most abundant infiltrating immune cell types found in tumors are macrophages. Macrophage infiltration is correlated with poor patient prognosis in over 80% of cancers analyzed (Bingle et al., 2002), and macrophages in tumors are generally polarized towards a tumor-promoting phenotype. Tumor-associated macrophages (TAMs) can promote cancer cell

invasion by producing growth factors such as epidermal growth factor (EGF) that increase the invasiveness of cancer cells, or by producing matrix-remodeling enzymes such as cysteine cathepsin proteases, matrix metalloproteinases and serine proteases (Joyce and Pollard, 2009). Depletion of macrophages leads to reduced tumor angiogenesis, at least partially through decreased production of angiogenic growth factors including vascular endothelial growth factor-A (VEGF-A) (Lewis and Pollard, 2006) and proteases such as cysteine cathepsins (Gocheva et al., 2010). In addition, TAMs can blunt response to chemotherapies and promote tumor rebound (DeNardo et al., 2011; Shree et al., 2011).

Tumor lymphangiogenesis

Regional lymph node metastasis is a common event in solid tumors and is considered a marker for dissemination, increased stage and worse prognosis across many tumor types (Sundar and Ganesan, 2007). It is still under debate whether tumor cells metastasize to other organs from the lymph nodes, or whether the presence of tumor cells in the lymph nodes is a reflection their intrinsic invasiveness. Therefore, the process of lymphatic invasion and metastasis to regional lymph nodes and whether tumors promote lymphangiogenesis in a manner similar to angiogenesis are still an open area of investigation.

Lymphatic vessels regulate tissue homeostasis by draining protein-rich fluid from the interstitial space and play an important role in immune surveillance.

Lymphatic capillaries are blind-ended and thin-walled vessels of approximately 30–80 μm in diameter and are composed of a single layer of lymphatic endothelial cells (LECs). In contrast to blood vessels, they have no pericytes or smooth muscle cells, have little or no basement membrane, exhibit endothelial gaps and display distinct gene expression patterns (Tammela and Alitalo, 2010). Vascular endothelial growth factor-C (VEGF-C) is an essential chemotactic and survival factor during lymphangiogenesis that, along with VEGF-D, signals through the VEGF receptor-3 (VEGFR-3). Additionally, it has been shown that in certain contexts, VEGF-A, fibroblast growth factor-2 (FGF-2), insulin-like growth factor 1 (IGF-1), IGF-2, hepatocyte growth factor (HGF), endothelin-1 (ET-1), and platelet-derived growth factor-B (PDGF-B) can induce lymphangiogenesis in a VEGFR-3 independent manner; however most of their effects are secondary to VEGF-C signaling (Tammela and Alitalo, 2010).

It is known that tumor cells enter the lymphatic vasculature by invading pre-existing lymphatic vessels in the tumor periphery or by eliciting lymphangiogenesis via growth factor production (Tammela and Alitalo, 2010). Consistently, it has been shown that overexpression of VEGF-C in breast, colorectal, gastric, thyroid, and prostate cancers is associated with poor prognosis and that the expression levels of VEGF-C (and less frequently VEGF-D) also strongly correlate with lymph node metastasis in more than 30 studies (Sundar and Ganesan, 2007). Studies in mice have since validated the importance of the VEGF-C/VEGFR-3 signaling axis. Overexpression of VEGF-C

in a breast cancer cell line increased intratumoral lymphangiogenesis, resulting in significantly enhanced metastasis to regional lymph nodes and to lungs (Skobe et al., 2001). Additionally, β -cell specific overexpression of VEGF-C in the RT2 model led to increased peritumoral lymphangiogenesis and increased lymph node metastasis, demonstrating that VEGF-C-induced lymphangiogenesis can mediate tumor cell dissemination and the formation of lymph node metastases (Mandriota et al., 2001).

Myeloid cells have also been shown to play an important role in lymphangiogenesis through their production of lymphangiogenic growth factors such as VEGF-C and VEGF-D, and through direct incorporation into lymphatic vessels in the context of inflammation. In a corneal transplantation model, newly formed lymphatic vessels originated from CD11b⁺ macrophages and expressed lymphatic-specific transcription factors (Maruyama et al., 2005). In humans, a retrospective study of sex-mismatched, rejected kidney transplants showed integration of recipient-derived cells into lymphatic vessels, constituting about 4.5% of all LECs in the rejected organ (Kerjaschki et al., 2006). In addition, *in vitro* differentiated macrophages are able to aggregate into lymphatic-like structures, gaining expression of LEC markers (Maruyama et al., 2005; Zumsteg et al., 2009). The contribution of bone marrow-derived cells (BMDCs) directly to tumor lymphangiogenesis remains very controversial. Studies using B16F1 melanoma and Lewis lung carcinoma cells injected into mice with genetically labeled bone marrow showed no integration of BMDCs into tumor-associated

lymphatic vessels (He et al., 2004). However, incorporation of BMDCs into lymphatic vessels has been observed in T241 fibrosarcoma tumors, the *Apc*^{Min/+} model of intestinal adenoma, the TRAMP-C1 prostate adenocarcinoma model and in the RIP1-VEGF-C; RT2 model (Jiang et al., 2008; Religa et al., 2005; Zumsteg et al., 2009).

Remodeling of the ECM during tumorigenesis

A large proportion of space occupied by and surrounding tumors is comprised of the extracellular matrix (ECM), a heterogeneous mix of proteins and polysaccharides, including heparan sulfate proteoglycans (HSPGs), collagen, laminin, and fibronectin, that form an intricate three-dimensional network (Kim et al., 2011). The ECM functions as a scaffold for cell and tissue organization and provides important biochemical cues affecting cell function. The ECM regulates various biological functions largely through its ability to bind other ECM proteins, growth factors, signal receptors and adhesion molecules. Remodeling of the ECM is a critical requirement during multiple stages of tumor development, facilitating cancer cell proliferation, angiogenesis, invasion, and metastasis.

Heparan sulfate

HSPGs are a key and abundant component of the ECM and consist of a protein core to which heparan sulfate side chains are covalently attached. HSPGs present in the matrix include perlecan, agrin, collagen type XI, syndecans and glypicans (Kim et al., 2011). Perlecan, agrin and collagens are actively secreted

into the ECM by epithelial cells and stromal cells including fibroblasts and osteoblasts. Syndecans and glypicans are found on the cell surface where they exert their function and can also be shed by proteases and phospholipidases (Brunner et al., 1994; Manon-Jensen et al., 2010). Heparanase is the only known endoglycosidase enzyme capable of heparan sulfate cleavage.

The ECM, and in particular HSPGs, play crucial and complex roles during growth factor receptor signaling. The heparan sulfate side chains bind to many growth factors, angiogenic proteins, and chemokines, allowing HSPGs to function as storage depots for these factors (Vlodavsky et al., 2012). Heparan sulfate-binding growth factors include the FGFs, VEGFs and transforming growth factor- β (TGF- β). The localization of growth factors by the ECM contributes to the establishment of gradients that play vital roles in developmental patterning and allows for increased local concentration of growth factors near to their cell surface receptors. These heparan sulfate-bound growth factors can then be released at an appropriate time by heparanase, such as during wound healing (Zcharia et al., 2005). In addition, heparan sulfate fragments produced by heparanase cleavage can function in receptor-ligand complex formation and enhance signaling of growth factors such as VEGF and FGF (Vlodavsky et al., 2012).

Heparanase cleaves HSPGs

Heparanase is an endo- β -glucuronidase that cleaves heparan sulfate side chains at specific intrachain sites, releasing saccharide fragments of 4-7 kDa. Mammals

express only one functional heparanase enzyme, heparanase-1, which for simplification will be referred to as heparanase (Hulett et al., 1999; Kussie et al., 1999; Toyoshima and Nakajima, 1999; Vlodavsky et al., 1999). Heparanase is a 61.2 kDa protein that is produced as a pro-enzyme that is post-translationally cleaved into 8 and 50 kDa fragments that non-covalently associate to form active heparanase (Levy-Adam et al., 2003). Cleavage and activation of heparanase is performed by the protease cathepsin L (Abboud-Jarrous et al., 2008). Similar to other glycosyl hydrolases, the catalytic mechanism of heparanase involves two conserved acidic residues, Glu²²⁵ and Glu³⁴³ (Hulett et al., 2000).

Normally, heparanase expression is repressed except for in platelets, mast cells, placental trophoblasts, keratinocytes and leukocytes (Vlodavsky et al., 2012). Wild-type p53 has been shown to inhibit heparanase transcription, and mutation of p53 has been shown to lead to heparanase activation. In addition, early growth response 1 (EGR1) has been implicated in inducible transcription of heparanase. Heparanase expression is stimulated by high glucose, reactive oxygen species, estrogens and inflammatory cytokines (Hermano et al., 2012).

Heparanase has also been described to have several non-enzymatic functions. Heparanase can interact with syndecans on the cell surface, inducing their clustering and can enhance cell spreading with activation of PKC, Src and Rac1 (Fux et al., 2009). In addition, it has been shown that heparanase can activate Akt, Src and p38 non-enzymatically, leading to downstream production of VEGF-

A, VEGF-C, tissue factor (TF) and cyclooxygenase 2 (COX2) (Fux et al., 2009). It has been shown through binding experiments that heparanase associates with low-affinity, high-abundance HSPGs and also with a high-affinity, low-abundance cell-surface receptor, that currently remains unknown (Ben-Zaken et al., 2008).

An additional homolog, heparanase-2 (Hpa2), has also been identified, however no enzymatic role for this enzyme has been identified (McKenzie et al., 2000). It has been recently discovered that Hpa2 can inhibit heparanase enzymatic activity, likely due to its high affinity for heparan sulfate and its ability to physically associate with heparanase (Levy-Adam et al., 2010).

Transgenic mice were created to interrogate the functions of heparanase. *Hpa*-Tg mice express the human heparanase transgene under the β -actin promoter, leading to constitutive overexpression and an increase in heparanase activity of 6- to 30-fold depending on the tissue examined (Zcharia et al., 2004). These mice were viable and fertile and exhibited a decrease in the size of heparan sulfate chains in adult tissues. Examination of most tissues revealed no morphological changes, except for increased mammary gland branching, more abundant alveoli and increased hair growth. Heparanase knock-out (*Hpse*^{-/-}) mice were also generated and found to be viable, fertile and exhibited an accumulation of long heparan sulfate chains (Zcharia et al., 2009). *Hpse*^{-/-} mice did not show any apparent anatomical abnormalities, most likely due to a

compensatory upregulation of matrix metalloproteinases observed in several organs such as the liver and kidney.

Heparanase induction has been reported in several inflammatory conditions, associated with degradation of heparan sulfate, remodeling of the ECM, release of inflammatory chemokines and facilitation of inflammatory cells migrating toward sites of injury (Hermano et al., 2012). Increased heparanase has been observed in rheumatoid arthritis, type 2 diabetes, ulcerative colitis and Crohn's disease. Heparanase is produced by infiltrating immune cells, and upregulated in epithelial cells and endothelial cells at the inflammatory site. Interestingly, in a mouse model of inflammatory bowel disease, heparanase was found to power a chronic inflammation circuit, in which heparanase was constantly overexpressed and activated by the epithelial cells (Lerner et al., 2011). This activates macrophages to produce inflammatory cytokines such as tumor necrosis factor- α (TNF- α), further stimulating epithelial production of heparanase.

Heparanase in tumor progression and metastasis

Some of the earliest studies of heparanase showed that its activity was associated with the metastatic potential of tumor cells such as B16 melanoma and T-lymphoma (Nakajima et al., 1983; Vlodaysky et al., 1983). Expression of heparanase has been shown to be upregulated in many tumor types including bladder, breast, colon, head and neck, lung, multiple myeloma and renal cancers (Vlodaysky et al., 2012). Additionally, it has been shown to be positively

correlated with increased microvascular density, tumor size, metastasis and decreased survival in many of these studies.

Overexpression and silencing of heparanase in cancer cell lines showed that heparanase enhances cell dissemination and promotes the establishment of a vascular network that accelerates primary tumor growth and provides a gateway for invading metastatic cells (Vlodavsky et al., 2012). During tumorigenesis, heparanase is thought to not only break down HSPGs within the ECM, but also to increase the bioavailability of growth factors. Therefore, the release of HSPG-bound growth factors such as VEGF is proposed to promote tumor angiogenesis.

It has been previously shown that heparanase is upregulated during multistage tumorigenesis in the RT2 model of pancreatic neuroendocrine tumorigenesis (Joyce et al., 2005). Treatment of RT2 mice with PI-88, a heparan sulfate mimetic, was used to inhibit both heparanase activity and heparan sulfate effector functions. PI-88 treatment impaired tumor cell proliferation and increased apoptosis, leading to a decreased tumor burden. In addition, invasion and tumor angiogenesis were significantly decreased, indirectly implicating heparan sulfate-mediated signaling and heparanase in regulating these processes. However, the specific functions of the heparanase enzyme itself in pancreatic neuroendocrine tumorigenesis were unknown.

Thesis aims

Pancreatic neuroendocrine tumors (PanNETs) are a rare but clinically challenging tumor type; a consequence of marked disease heterogeneity and limited understanding of the molecular basis for these cancers. Therefore, the objective of my thesis research was to identify tumor cell intrinsic and extrinsic regulators of PanNET tumorigenesis.

In Chapter 3, I describe my research into the roles of heparanase in PanNET tumorigenesis. We found that heparanase has both tumor cell intrinsic and extrinsic functions in promoting tumor progression. We have found that heparanase expression is significantly correlated with increased malignancy and metastasis in PanNET patients. We genetically manipulated heparanase levels in the RT2 model using heparanase transgenic mice, which constitutively overexpress heparanase, or heparanase knockout mice, and identified critical roles for both macrophage- and cancer cell-derived heparanase in promoting tumor invasion. Additionally, we showed that elevated heparanase activity induces tumor lymphangiogenesis and promotes the trans-differentiation of macrophages into lymphatic endothelial cell-like structures. Together, our findings demonstrate a multifaceted role for heparanase in supporting various processes critical to PanNET progression, and thus implicate heparanase as a potential prognostic factor and attractive therapeutic target for PanNET patients.

I also describe my research on the identification and characterization of a subset of RT2 tumors that mimic PD-PanNETs, which we termed poorly differentiated invasive carcinomas (PDIC). Through analysis of markers of neuroendocrine differentiation we find that PDICs are intrinsically different than insulinomas, exhibiting loss of differentiation markers, a high proliferative index and selective expression of the Id1 (inhibitor of DNA-binding 1) protein. We are currently using the specific expression of Id1 to generate a mouse model of PD-PanNET tumorigenesis. The insights gained into the molecular mechanisms of tumorigenesis in this tumor type, and the use of this model as a preclinical screening tool for therapeutics, will allow us to make important advances in a tumor type that is poorly understood. This research is described in Chapter 4.

CHAPTER TWO

Materials and Methods

Transgenic mice

The generation and characterization of RIP1-Tag2 (Hanahan, 1985), heparanase transgenic (*Hpa-Tg*) (Zcharia et al., 2004), and heparanase knockout (*Hpse*^{-/-}) (Zcharia et al., 2009) mice have been previously reported. *Hpse*^{-/-} and *Hpa-Tg* mice were backcrossed to the C57BL/6 background for at least 10 generations. β -Actin GFP transgenic mice (Okabe et al., 1997) in the C57BL/6 background were purchased from Jackson Laboratories. Rosa26^{LSL-LacZ} and Rosa 26^{LSL-YFP} mice were previously reported (Soriano, 1999; Srinivas et al., 2001). Id1^{IRES-creERT2} mice were generated and provided by R. Benezra (Nam and Benezra, 2009). Mice were treated with tamoxifen by injecting 4mg tamoxifen (200 μ L of stock at 20mg/mL dissolved in corn oil, Sigma) intraperitoneally for 5 days.

Bone marrow transplantation (BMT) protocol

Bone marrow was harvested from WT, *Hpa-Tg* or *Hpse*^{-/-} β -actin-GFP mice by flushing the femurs and tibias with X-VIVO 20 medium (Cambrex). The flushed cells were resuspended in PBS and 1×10^6 nucleated cells were injected through the tail veins of 4 week old lethally irradiated (950 rads) WT or *Hpa-Tg* RT2 animals. *Hpa-Tg* mice were given soft food and Sulfatrim antibiotic diet for 3-4 weeks after transplantation. After 4 weeks, recipient mice were bled from the orbital sinus to evaluate BM transplantation efficiency by determining the

percentage of GFP⁺ cells using flow cytometry. Mice were subsequently aged to 13.5 weeks for calculation of tumor volume and analysis of the tumor phenotype.

Tissue processing and analysis

RT2 mice were sacrificed by heart perfusion with PBS followed by 10% zinc-buffered formalin. Tumor-containing pancreas and control tissues were removed, placed in 30% sucrose overnight and embedded in OCT (Tissue-Tek) or were formalin-fixed overnight, processed through an ethanol series and embedded in paraffin blocks. Lesions greater than 1 mm x 1 mm were counted as tumors. Tumor burden was represented as the sum of the volumes of all tumors per mouse and calculated using the formula: volume = width² x length x 0.52 to approximate the volume of a spheroid. Frozen sections (10 μm or 35 μm thickness) were cut on a cryostat and paraffin sections (5 μm) were cut on a microtome. For invasion grading, hematoxylin and eosin (H&E) staining was performed and the lesions were graded as previously described (Lopez and Hanahan, 2002), following a double-blind protocol and independently assessed by two investigators (K.E.H and J.A.J.).

Immunohistochemistry (IHC) and immunofluorescence (IF) staining

For immunofluorescence staining on 10 μm-thick frozen sections, slides were blocked with 1X PNB-blocking buffer (Perkin Elmer), incubated with the primary antibody of interest overnight at 4°C, incubated with the corresponding

fluorescently-tagged secondary antibody for 1 hour at room temperature (RT), incubated with 46-diamidino-2-phenyl indole (DAPI) for 10 minutes and mounted with ProLong Gold (Invitrogen). For immunofluorescence on 35 μ m sections, slides were permeabilized with 0.3% TritonX, blocked with 5% goat serum, incubated with primary antibodies overnight at RT, incubated with corresponding fluorescently-tagged secondary antibody for 4.5 hours at RT, incubated with DAPI for 20 minutes and mounted with ProLong Gold. Species-matched immunoglobulins were used as negative controls. Paraffin sections were stained using DAB detection with a Discovery XT automated staining processor (Ventana Medical Systems, Inc). Tissue sections were visualized under a Carl Zeiss Axioimager Z1 microscope equipped with an Apotome. The following antibodies were used for immunofluorescence: rabbit anti-LYVE-1 (Abcam, 1:500), rat anti-F4/80 (Serotec, 1:1000), Syrian hamster anti-podoplanin (AngioBio, 1:500), rat anti-MECA32 (BD, 1:100), rabbit anti-NG2 (Chemicon, 1:200), pEGFR (Tyr 1068, Cell Signaling, 1:500). The following antibodies were used for DAB staining: mouse anti-HS (10E4, Seikagaku Corp 1:200), rabbit anti-SV40 T antigen (Santa Cruz, 1:500), rabbit anti-human heparanase (gift from I.Vlodavsky, 1:500; (Cohen-Kaplan et al., 2008)), guinea pig anti-insulin (DAKO, 1:1000), rabbit anti-synaptophysin (DAKO, 1:200), rabbit anti-Ki67 (Vector, 1:200), rabbit anti-chromogranin A (Abcam 1:250), rabbit anti-MafA (Abcam, 1:500), anti-Nkx6.1, rabbit anti-Pdx1 (Abcam, 1:500), rabbit anti-glucagon (Millipore 1:1000), rabbit anti-somatostatin (DAKO, 1:500), rabbit anti Id-1 (BioCheck, 1:200), rabbit anti-Id3 (BioCheck, 1:200), and chicken anti- β galactosidase (Abcam, 1:500).

IHC and IF tissue analysis

For intrapancreatic lymph node metastasis analysis, paraffin blocks from mice at 13.5 weeks of age were serially sectioned through the whole pancreas and every 10th slide was stained for T antigen. For liver metastasis analysis, paraffin blocks containing whole livers from mice at 16 weeks of age were serially sectioned 500 µm into each tissue and every 10th slide was stained for T antigen. Stained tissue sections were acquired using TissueFAXS software (TissueGnostics). PDICs were identified by serially sectioning paraffin blocks containing pancreas of RT2 mice at 13.5 weeks of age and staining every 10th section for insulin. PDIC status was confirmed by staining with Id1. Lymphangiogenesis analysis was performed on 35 µm sections using MetaMorph software (Molecular Devices) using a dilated peri-tumoral region, 500 µm in diameter, to calculate the total LYVE-1⁺ area and the total DAPI⁺ area within this region with using an in-house macro written by the MSKCC Molecular Cytology Core Facility. Analysis of tumor vasculature was performed by calculating total MECA32 area, total DAPI area and the area of NG2 that overlapped MECA32 with MetaMorph analysis software, using an in-house macro written by the MSKCC Molecular Cytology Core Facility.

Assay for trans-differentiation of BMDM into LEC-like structures

Femurs and tibiae from WT or *Hpa*-Tg mice, in the C57BL/6 background, were harvested under sterile conditions from both legs and flushed using a 25-gauge needle. The marrow was passed through a 40 µm strainer and cultured in 30 mL

Teflon bags (PermaLife) with 10 ng/mL recombinant mouse colony stimulating factor (CSF)-1 (R&D Systems). Bone marrow cells were cultured in Teflon bags for 7 days, with fresh CSF-1-containing medium replacing old medium every other day to induce macrophage differentiation. Matrigel (Becton Dickenson) and endothelial cell media EGM-2 MV (Lonza) were mixed 1:1 and plated on 24-well or 96-well plates for 1 hour at 37°C. Bone marrow-derived macrophages (BMDM) were collected and either 8×10^4 (96-well) or 5×10^5 (24-well) cells were plated per well in EGM-2 supplemented with 1 μ g/ml LPS. After 8 days of culture, cells were isolated by washing with ice cold PBS and lysing in TRIzol reagent (Invitrogen) for RNA isolation. For assays with growth factor addition, BMDM were plated with 4 replicates in 96-well plates with EGM-2 supplemented with either 100 ng/ml mouse VEGF-A¹⁶⁴ (R&D), mouse VEGF-C (Sigma), mouse FGF-2 (R&D), or mouse HGF (R&D) and replenished at day 3 of culture. At day 8 of culture, wells were visualized and number of lymphatic endothelial cell (LEC)-like structures were counted and normalized within each experiment. Immunofluorescence analysis of LEC-like structures was performed on cultures at day 8 using DAPI, anti-podoplanin and anti-F4/80 antibodies.

Flow cytometry and sorting

Tumors were isolated and processed for fluorescence-activated cell sorting as previously described (Pyonteck et al., 2012) using the following antibodies: CD31-FITC (1:100, BD Pharmingen), CD45-PE (1:200, BD Pharmingen), anti-F4/80-APC (1:100, Serotec) and 46-diamidino-2-phenyl indole (DAPI) for dead

cell exclusion. The cells were sorted on a fluorescence-activated cell sorting Aria flow cytometer (BD Biosciences) and several fractions collected: a mixed population of live cells (DAPI⁺); purified tumor cells (DAPI⁻CD31⁻CD45⁻F4/80⁻); macrophages (DAPI⁻ CD45⁺ F4/80⁺) and endothelial cells (DAPI⁻CD31⁺).

RNA isolation and qRT-PCR

RNA was prepared from samples using TRIzol reagent and subsequently DNase-treated (Invitrogen) according to the manufacturers instructions. cDNA was synthesized using the First Strand cDNA Synthesis Kit for RT-PCR (Roche). Real-time qPCR was performed on cDNA samples using the ABI 7900HT Fast Real-Time PCR system. Primers for ubiquitin C (Mm01201237_m1), CD68 (Mm03047343_m1), CD31 (Mm00476702_m1), heparanase (Mm00461768_m1), SV40 T-antigen (T-Ag, custom probe), LYVE-1 (Mm00475056_m1), podoplanin (Mm00494716_m1), VEGFR-1 (Mm00438980_m1), VEGFR-2 (Mm01222419_m1), VEGFR-3 (Mm01292604_m1), VEGF-A (Mm00437304_m1), VEGF-C (Mm01202432_m1), VEGF-D (Mm01131929_m1), FGF-2 (Mm00433287_m1), HGF (Mm01135193_m1), Id1 (Mm00775963_g1), synaptophysin (Mm00437606_s1), Ins2 (Mm00731595_gH), MafA (Mm00845209_s1), Ngn3 (Mm00845209_s1) HPRT1 (Hs99999909_m1) and human heparanase (Hs00180737_m1) were purchased from Applied Biosystems.

Western blotting

Protein lysates were made from dissected RT2 tumors using RIPA lysis buffer. 40 µg of protein was loaded onto SDS-PAGE gels and transferred to PVDF membranes for immunoblotting. Membranes were probed with antibodies against Id1 (BioCheck 1:500), insulin (DAKO 1:1000), MafA (Abcam 1:1000) and actin (Sigma, 1:5000) and detected using HRP-conjugated anti-guinea pig or anti-rabbit (Jackson ImmunoResearch) antibodies using chemiluminescence detection (Amersham).

Tumor cell line infections

Lentivirus was produced using 293T cells, with a PWPI-Id1 vector or a PWPI-empty vector (gift from L. Barrett and R. Benezra). The β-tumor cell line 916-1 was infected with this lentivirus with the addition of 8 µg/mL polybrene. After passaging, cells were FACS sorted based on GFP expression to select for infected cells and were cultured for two more passages and subsequently analyzed for gene expression.

Human PanNET samples

Two tissue microarrays (TMAs) were constructed from archival paraffin-embedded tissue from a series of >150 PanNETs surgically resected from patients at MSKCC. Patient anonymity was ensured, and the study was performed in compliance with the Institutional Review Board. Three 0.6 mm

tissue cores were punched from representative areas of the donor block and embedded in a recipient block using an automated TMA machine. Five μm tissue sections were cut from this TMA and stained for heparanase and scored double-blindly by K.E.H and J.A.Joyce.) as negative (0) or positive [three levels: weak (1); moderate (2); strong (3)], based on staining intensity and percentage of cells that stained positive. Heparanase staining was then correlated to clinicopathological parameters including AJCC tumor stage (Edge and Compton, 2010), tumor grade (low: <2 mitoses/50 high power field (HPF); intermediate: ≥ 2 mitoses/50 HPF; high grade: >50 mitoses/50 HPF) (Ferrone et al., 2007) and the number of mitoses per 50 HPFs scored by L.Tang. Samples with incomplete patient data were excluded from the respective analysis. RNA was obtained from PanNETs in patient-matched primary and liver metastases as previously described (Hu et al., 2010). Normal islet RNA was isolated from snap frozen cultured human islets from healthy organ donors (Cell Transplant Center, Diabetes Research Institute, University of Miami School of Medicine).

Statistical analysis

Throughout this study, means \pm SEM (standard error of the mean) are reported unless otherwise specified. For all two-way comparisons, unpaired t-tests or Mann-Whitney tests where indicated were used and were considered statistically significant if $P < 0.05$. A cumulative logit model (McCullagh, 1980) with generalized estimating equations to correct for correlations within individual mice was used to compare the distribution of tumor grades in RT2 mice. For TMA analysis of tumor

stage, tumor grade, and distant metastasis, Fisher's exact test was used. For comparison of mitosis, one-way ANOVA was used.

CHAPTER THREE

Heparanase Promotes Tumorigenesis in PanNETs

Remodeling of the ECM is a critical requirement during multiple stages of tumorigenesis, facilitating cancer cell proliferation, angiogenesis, invasion and metastasis. One of the most abundant types of macromolecules within the ECM are HSPGs, which function as a scaffold for cell and tissue organization and provide important biochemical cues affecting cell function. HSPGs, in particular, play crucial and complex roles during growth factor receptor signaling. The heparan sulfate side chains bind to many growth factors, angiogenic proteins, and chemokines, allowing HSPGs to function as storage depots for these factors (Vlodavsky et al., 2012). In addition, the heparan sulfate fragments produced upon cleavage can function in receptor-ligand complex formation to enhance growth factor signaling. Cleavage of the heparan sulfate side chains is performed by one enzyme in mammals, heparanase. Heparanase activity can thus lead to physical remodeling of the ECM, to release growth factors tethered within the matrix and increase their bioavailability and thus enhance growth factor signaling.

The endoglycosidase heparanase has been shown to be upregulated in many tumor types and to be correlated with increased malignancy, metastasis and microvascular density in numerous studies (Vlodavsky et al., 2012). Studies with cancer cell lines have shown that heparanase expression enhances metastatic spread and induces angiogenesis. In addition, a previous study in the RT2 model

showed that heparanase is upregulated during tumor progression and treatment with PI-88, a heparan sulfate mimetic that inhibits both heparanase activity and heparan sulfate effector functions, leads to decreases in tumor growth, angiogenesis, and tumor invasion. While this indirectly implicates heparan sulfate-mediated signaling and heparanase in these processes, the specific functions of the heparanase enzyme itself in pancreatic neuroendocrine tumorigenesis were unknown. Therefore, we sought to evaluate the importance of heparanase in promoting PanNET tumorigenesis using patient samples and to elucidate the specific roles of heparanase using the RT2 model of PanNETs.

Results

Heparanase expression is associated with malignant progression in human pancreatic neuroendocrine tumors

To investigate whether heparanase is expressed in PanNETs, we first performed immunohistochemistry for heparanase on PanNET patient tissue samples and on normal islet samples. While normal islets had minimal heparanase staining, tumors exhibited heparanase staining that varied in intensity. We then obtained tissue microarrays (TMAs) with samples from over 150 patients with PanNETs, performed immunohistochemistry for heparanase, and blindly scored for staining intensity on a 0 (no staining) to 3 (high staining) scale (Figure 3.1A). Comparing staining intensity with patient clinicopathological data revealed a significant correlation between increased heparanase staining score and higher tumor stage, as classified by the American Joint Committee on Cancer (AJCC) staging

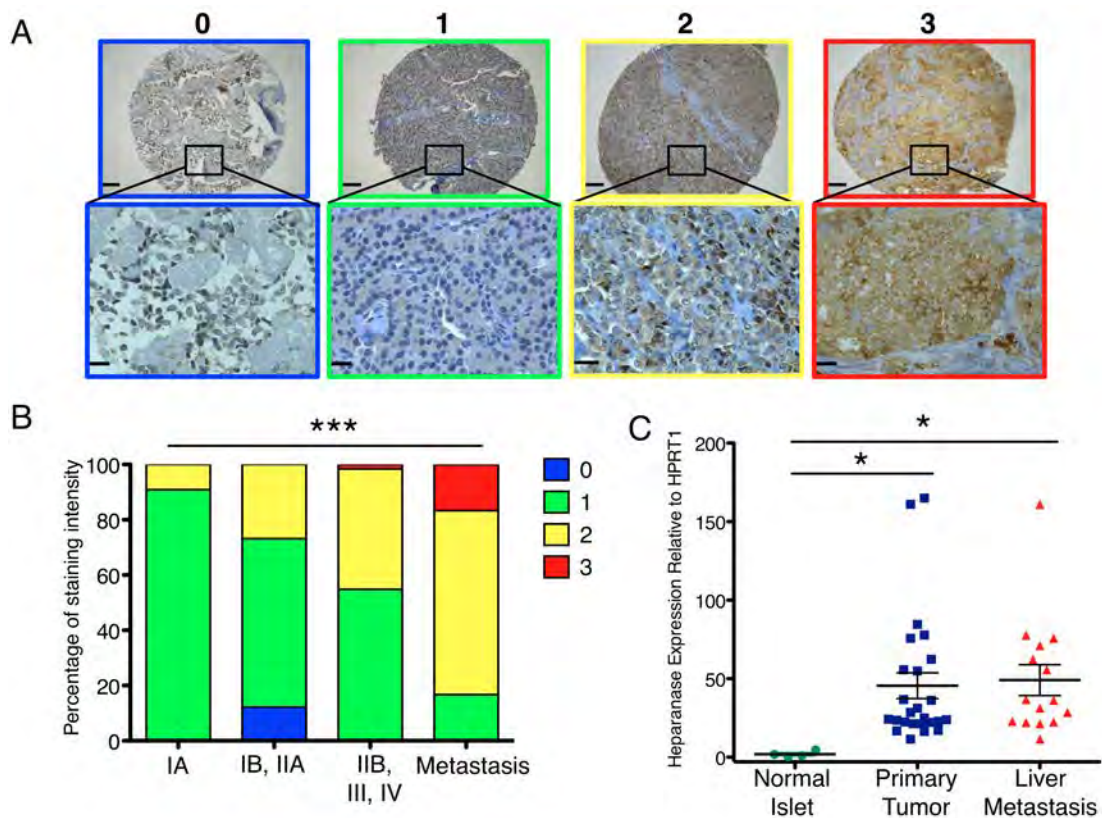


Figure 3.1. Heparanase expression is associated with malignant progression in human pancreatic neuroendocrine cancers. (A) Representative images for heparanase staining in TMAs constructed from PanNET patient samples. Heparanase staining intensity was scored on a 0 (absent staining) to 3 (high staining) scale. Scale bar for tissue sample overview: 100 μ m, scale bar for inset: 20 μ m. (B) Correlation of heparanase score with tumor stage by American Joint Cancer Committee (AJCC) staging manual 7th edition (Edge and Compton, 2010); see Table 3.1 for detailed patient information, *** P <0.0001. (C) Heparanase expression, normalized to HPRT1, in mRNA from normal islets ($n=4$), primary tumors ($n=25$) and liver metastases ($n=15$) from PanNET patients. Heparanase was significantly upregulated in primary tumors ($*P=0.046$) and liver metastases ($*P=0.026$) compared to normal islet samples.

Table 3.1: Comparison of clinical and histopathologic parameters associated with increased levels of heparanase immunostaining in PNET patients shown in Figure 3.1.

Clinicopathological parameters	n	Heparanase score			P value*
		0	1	2	
Tumor grade					0.008
Low	87	6	64	17	0
Intermediate	77	4	39	33	1
High	3	0	1	2	0
Staging (AJCC Stage)					<0.0001
IA	22	0	20	2	0
IB, IIA	82	10	50	22	0
IIB, III, IV	61	0	33	27	1
Metastasis	6	0	1	4	1
Mitosis (per 50 HPFs)		1.5 ± 1.5	4.1 ± 1.6	10.85 ± 3.5	2.0
Distant metastasis					
No metastasis	131	10	86	34	1
Distant metastasis	37	0	19	18	0

* The P values were calculated by one-way ANOVA for mitosis, and by Fisher's exact test for the other parameters. Significant P values are indicated in bold.

manual 7th edition (Edge and Compton, 2010) and highest levels of heparanase staining in tumors that had metastasized to the lymph nodes or the liver (Figure 3.1B). We also saw a significant correlation between increased heparanase staining and higher tumor grade as defined by tumor mitotic activity (Ferrone et al., 2007; Nolan-Stevaux et al., 2010) (Table 3.1). Additionally, we found that increased heparanase staining score was significantly correlated with the presence of distant metastasis based on patient records (Table 3.1).

As we had seen highest levels of heparanase staining in metastatic samples, we were thus interested in whether heparanase was upregulated during the metastatic process. In collaboration with Dr. Laura Tang in the MSKCC Pathology department, we obtained RNA from patient matched samples of primary tumor and liver metastases, the most common metastatic site in PanNET patients. We also obtained normal islet cell RNA from healthy donors. When comparing heparanase expression in tumors to normal islets, we found that heparanase was significantly upregulated by approximately 40-fold and was similarly highly expressed in matched metastatic tumors (Figure 3.1C). Therefore, heparanase is significantly upregulated in primary tumor samples and remains highly expressed in metastases. Together, these data show that heparanase can function as a prognostic indicator for the aggressiveness of the primary tumor and distant metastasis in PanNET patients.

Genetic manipulation of heparanase levels in the RIP1-Tag2 PanNET model

As we had established that there is a significant association between heparanase expression and increased malignancy and metastatic disease in PanNET patients, we were interested in determining the specific roles that heparanase may play in promoting pancreatic neuroendocrine tumorigenesis. We sought to investigate the roles of heparanase during spontaneous tumorigenesis by genetically manipulating its level of expression in the RT2 mouse model of islet cell carcinoma by crossing them to either heparanase transgenic (*Hpa-Tg*) or heparanase knock-out (*Hpse^{-/-}*) mice (Zcharia et al., 2009; Zcharia et al., 2004). When we analyzed end-stage mice at 13.5 weeks of age, we found that heparanase overexpression or deletion had no significant effect on tumor burden, assessed by both tumor size and tumor number (Figure 3.2). Therefore, modulating levels of the heparanase enzyme does not appear to impact tumor initiation or tumor growth.

We then sought to determine whether we could observe the effects of heparanase manipulation by staining tissue sections for heparan sulfate using the anti-heparan sulfate antibody 10E4. When examining the interior of tumors, heparan sulfate staining was primarily localized to blood vessels, which was expected, as HSPGs are an abundant component of the basement membrane (Figure 3.3A). The amount of staining was reduced in *Hpa-Tg* RT2 mice, indicative of increased heparan sulfate turnover through processing by heparanase. Consistent with this, we saw increased heparan sulfate

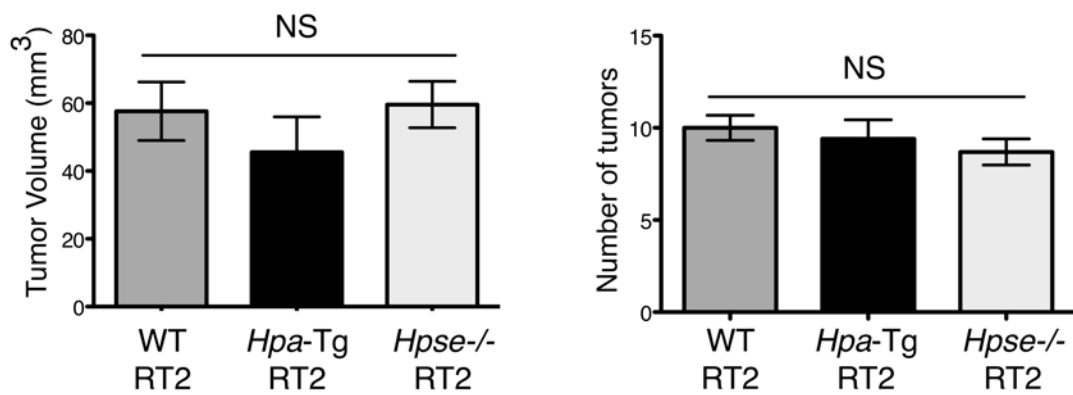


Figure 3.2. Genetic modulation of heparanase does not impact tumor burden in RT2 mice. Tumor volume and tumor number was determined in WT RT2 ($n=40$), *Hpa-Tg* RT2 ($n=25$) and *Hpse*^{-/-} RT2 ($n=26$) mice at 13.5 weeks of age. There was no significant (NS) difference in tumor burden for either genotype compared to WT RT2.

accumulation along blood vessels in *Hpse*^{-/-} RT2 mice. Interestingly, when examining the invasive fronts of wild-type (WT) RT2 tumors, we observed reduced levels of HS, similar to that observed in *Hpa*-Tg RT2 mice, suggesting that heparanase was active at invasive edges in these tumors and degraded HS during the process of matrix remodeling.

Heparanase promotes pancreatic neuroendocrine tumor invasion

The increased heparan sulfate turnover at invasive tumor fronts led us to investigate whether genetic manipulation of heparanase levels affected tumor invasion. Tumors were graded histologically into three classes of invasiveness: encapsulated tumors, microinvasive tumors (IC1), and invasive carcinomas (IC2) (Lopez and Hanahan, 2002). While the total number of tumors did not change in any of the genotypes (Figure 3.2), *Hpa*-Tg RT2 mice had significantly more invasive tumors compared to WT RT2 mice, with a striking 2.5-fold increase in the most invasive IC2 tumors (Figure 3.3B). Conversely, deletion of heparanase led to significantly less invasive tumors, consistent with an important role for heparanase in promoting tumor invasion (Figure 3.3B).

Given our findings that increased heparanase expression is significantly correlated with metastasis in PanNET patient samples and increased tumor invasion in a PanNET mouse model, we next investigated whether heparanase could alter the incidence of metastases in these mice. The RT2 model

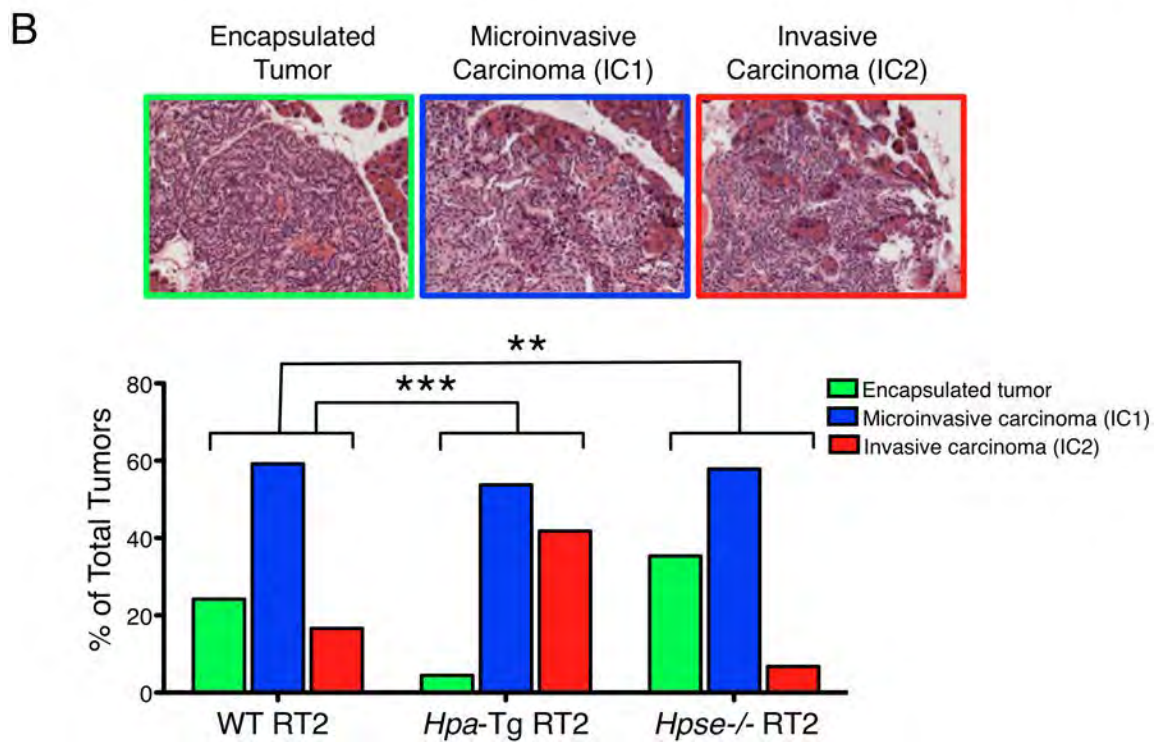
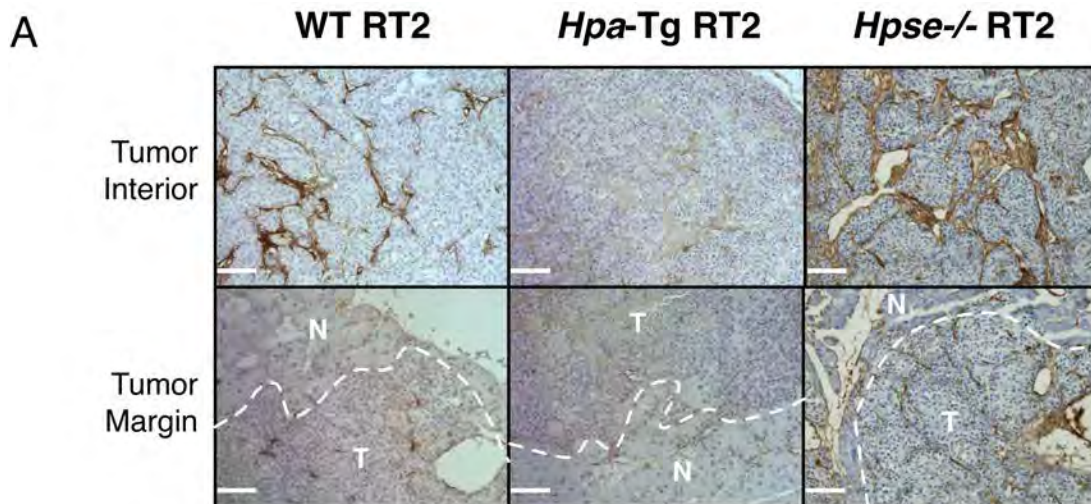
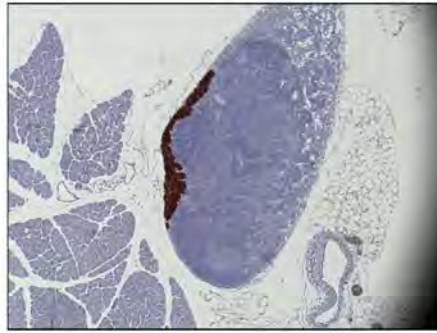
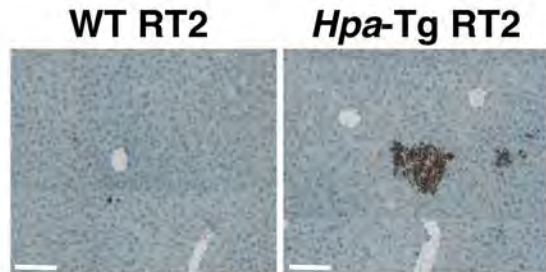


Figure 3.3. Heparanase enhances tumor invasion. (A) Paraffin sections of WT RT2, *Hpa*-Tg RT2 and *Hpse*^{-/-} RT2 mice were stained for heparan sulfate (brown). Scale bar 50 μ m. White dotted line indicates the margin between the tumor (T) and surrounding normal (N) pancreas. (B) H&E staining was used to grade tumors in WT RT2 ($n=30$), *Hpa*-Tg RT2 ($n=10$) and *Hpse*^{-/-} RT2 ($n=10$) mice. The relative proportions of encapsulated, microinvasive (IC1), and invasive carcinomas (IC2) were graphed. There is a significant increase in invasion in *Hpa*-Tg RT2 mice compared to WT RT2 ($***P<0.001$) and a significant decrease in invasion in *Hpse*^{-/-} RT2 mice ($**P=0.004$).

A

Genotype	LN Metastasis
WT RT2	4/10
<i>Hpa-Tg</i> RT2	4/10
<i>Hpse</i> ^{-/-} RT2	4/10

B

Genotype	Metastases >50 μ m
WT RT2	0/7
<i>Hpa-Tg</i> RT2	2/7

Figure 3.4. (A) Representative images of intrapancreatic lymph nodes with a synaptophysin-positive metastasis. All genotypes exhibited lymph node metastases in 40% of mice. (B) Representative images of T antigen-positive liver metastases in WT RT2 and *Hpa-Tg* RT2 mice. Two out of seven *Hpa-Tg* RT2 mice exhibit metastases larger than 50 μ m. T antigen was detected by DAB staining (brown) with a hematoxylin counterstain. Scale bar 50 μ m.

metastasizes with low frequency to the intrapancreatic lymph nodes and the liver; however, these mice generally succumb to hypoglycemia due to the production of insulin by the primary insulinomas before extensive metastasis can occur. We examined the liver and lymph nodes for the presence of metastases by serially sectioning tissues and staining for the tumor cell-specific markers T-antigen or synaptophysin. Analysis of the intrapancreatic lymph nodes at 13.5 weeks revealed that 40% of mice across all three genotypes had at least one lymph node metastasis, visualized by synaptophysin staining (Figure 3.4A). To allow for the further assessment of metastatic burden, we aged mice to 16 weeks, examined the livers of these mice and found single cells or small clusters of metastatic tumor cells that were present across all genotypes (Figure 3.4B). However, two of seven *Hpa-Tg* mice had a higher metastatic burden, with micrometastases that were larger than 50 μm (Fig. 2D), which were never observed in the other genotypes. Therefore, consistent with the PanNET patient results discussed above, these findings support the notion that overexpression of heparanase promotes metastatic outgrowth in PanNETs.

Macrophage supplied heparanase promotes tumor invasion

As we have established that heparanase plays an important role in promoting tumor invasion, we were interested in further characterizing which cell types within the tumor microenvironment were a source of heparanase. We performed fluorescence-activated cell sorting (FACS) on tumors from WT RT2 mice, and isolated cancer cells, tumor-associated macrophages (TAMs), and endothelial

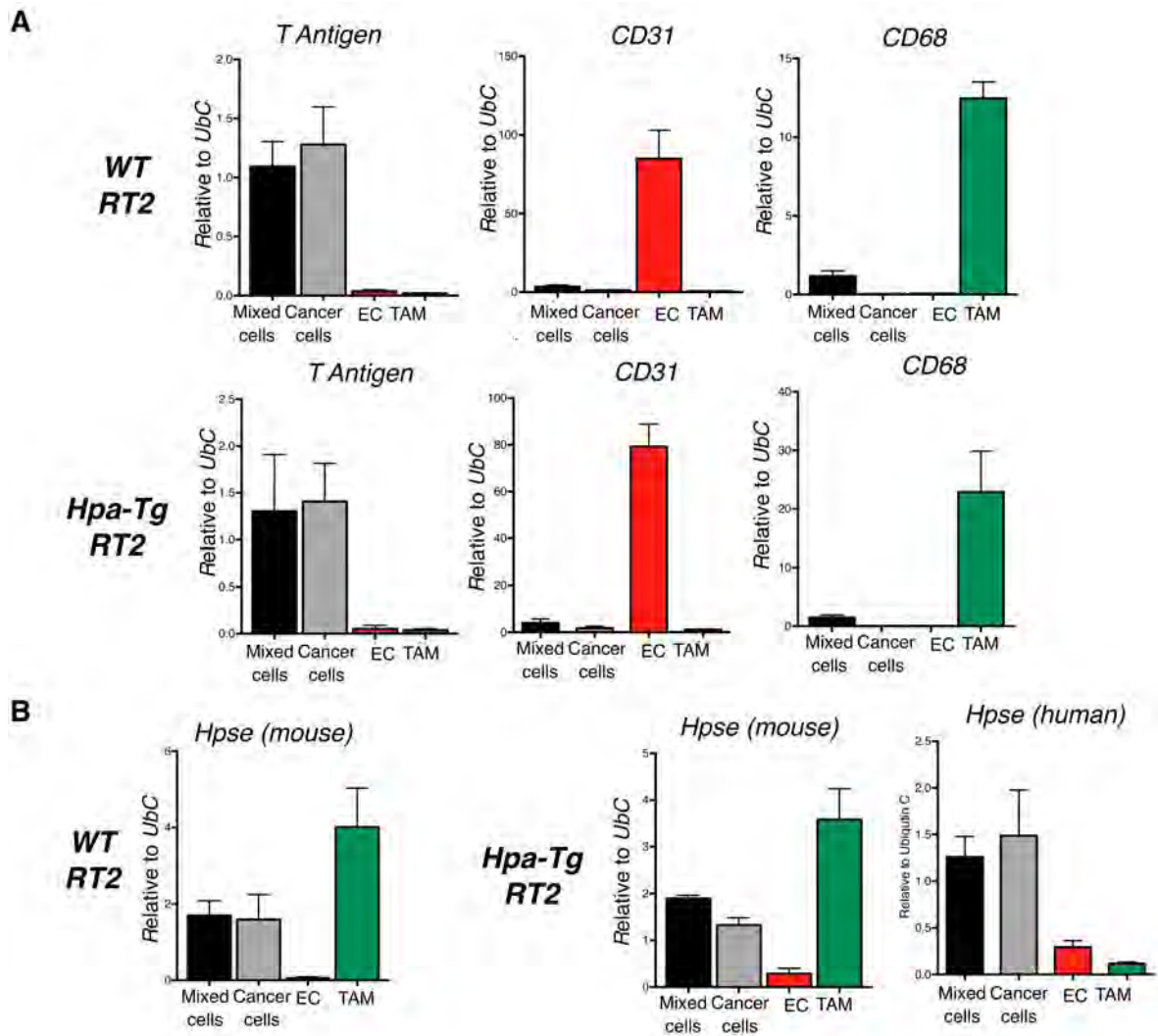


Figure 3.5. Heparanase expression is enriched in TAMs. (A) WT RT2 and *Hpa-Tg* tumors were sorted by flow cytometry into total mixed cells, cancer cell, endothelial cell (EC) and tumor-associated macrophage (TAM) fractions. Expression of T antigen (tumor cells), CD31 (endothelial cells) and CD68 (macrophages) were determined by qPCR to validate the purity of the sort. (B) Expression of mouse heparanase in WT RT2 samples and both mouse and human heparanase in *Hpa-Tg* RT2 samples was determined by qPCR. All gene expression data was normalized relative to Ubiquitin C (Ubc) levels. $n=4$ independent experiments.

cell populations. We confirmed the purity of the sort by performing qPCR for the following markers: T antigen for cancer cells, CD31 for endothelial cells and CD68 for TAMs and found that each marker was expressed exclusively in the appropriate cell population (Figure 3.5A). Analysis of heparanase expression revealed that both cancer cells and TAMs are a source of heparanase in WT RT2 mice, with a 2.5-fold enrichment in TAMs (Figure 3.5B).

We also performed sorts on *Hpa*-Tg RT2 tumors and confirmed the purity of the sorted cell populations (Figure 3.5A). We found that the expression of the endogenous mouse heparanase followed the same pattern as WT RT2 mice, with expression in cancer cells and enriched expression in TAMs (Figure 3.5B). Evaluation of the expression of the human heparanase transgene in the sorted samples revealed highest expression levels in cancer cells, with relatively lower levels in TAMs, although the amplification cycle number indicated that the expression in TAMs was still high.

Cancer cell- and TAM-supplied heparanase promote tumor invasion

While we have determined that heparanase is expressed at high levels in TAMs, it was unknown whether this TAM-supplied heparanase was promoting tumor invasion. To functionally test the importance of heparanase in TAMs versus cancer cells, we undertook bone marrow (BM) transplantation studies. As previous work has shown that in the RT2 model, 88% of BM-derived cells (BMDCs) found in tumors are TAMs (Gocheva et al., 2010), BM transplantation

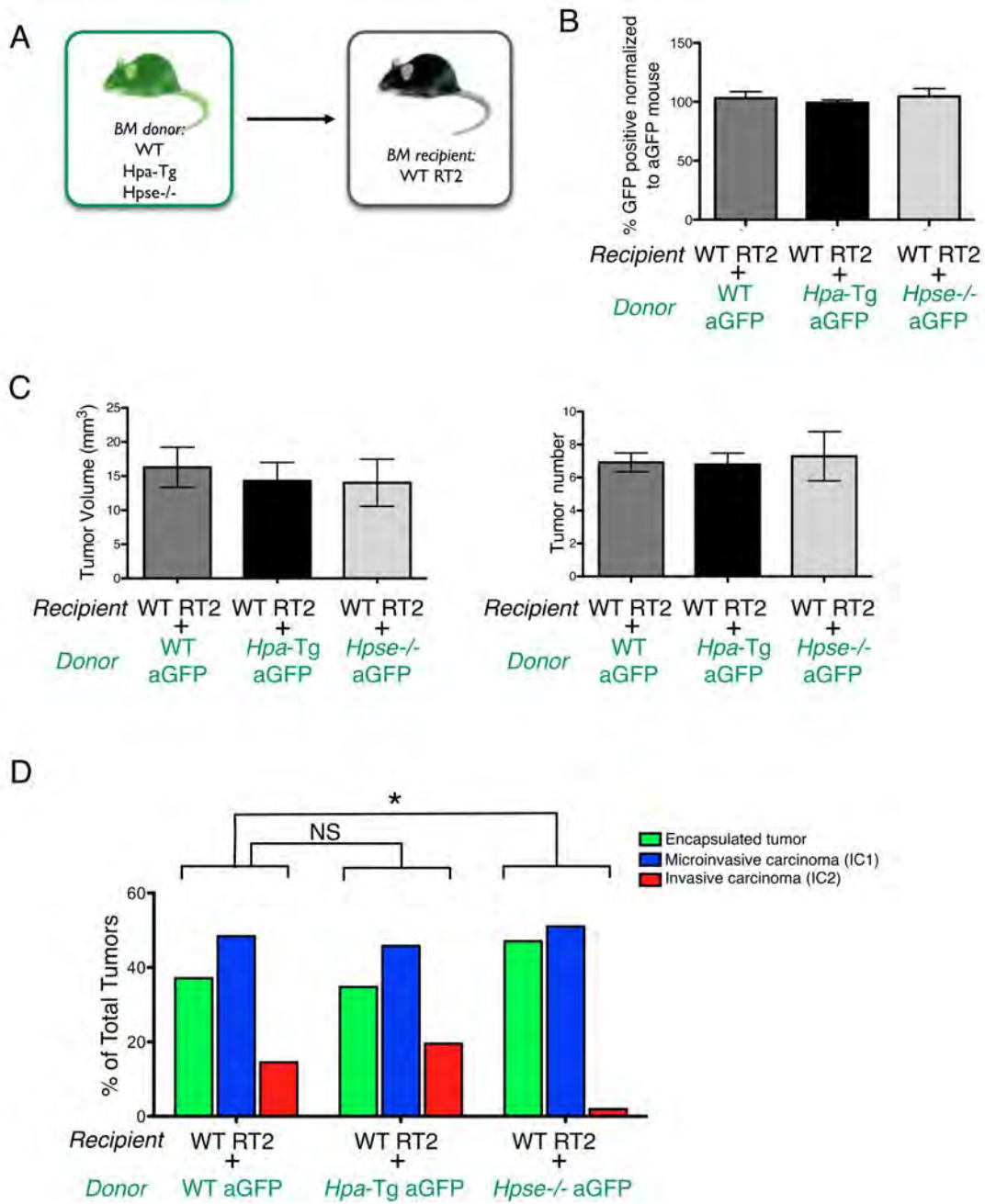


Figure 3.6. Heparanase promotes tumor invasion through both cancer cell- and TAM-derived sources. (A) Schematic of bone marrow transplantation experiments. (B) Engraftment of GFP⁺ positive BM was determined using flow cytometry 4-6 weeks after transplantation. The percentage of GFP⁺ bone marrow cells was normalized to an aGFP mouse. There was no impairment of *Hpa*-Tg and *Hpse*^{-/-} BM in engraftment. *n*=7-10 mice. (C) Tumor burden of BMT mice. Both tumor volume and tumor number were determined and no difference was seen between the experimental groups. (D) H&E staining was used to grade tumors following bone marrow transplantation of WT aGFP (*n*=10), *Hpa*-Tg aGFP (*n*=13) or *Hpse*^{-/-} aGFP (*n*=7) BM into WT RT2 mice. There was a significant decrease in tumor invasion in *Hpse*^{-/-} BM transplanted into WT RT2 mice (**P*=0.02). NS= not significant.

provides a means to genetically manipulate TAM-supplied heparanase levels in RT2 tumors. We transplanted BM isolated from either *Hpa-Tg* or *Hpse*^{-/-} mice, which were also positive for actin-GFP (a-GFP), into lethally irradiated WT RT2 mice at 4 weeks of age, before islet hyperproliferation has begun (Figure 3.6A). Engraftment of the BM was analyzed 4-6 weeks after transplantation and all experimental groups showed complete engraftment (Figure 3.6B). We then aged mice to 13.5 weeks and analyzed for tumor burden and tumor invasion.

As observed in the non-BMT genotypes described above (Figure 3.2), there was no impact of the different heparanase genotypes on tumor burden (Figure 3.6B). However, when analyzing tumor invasion in these mice, we found that transplantation of *Hpse*^{-/-} BM into WT RT2 mice significantly decreased tumor invasion as compared to the WT BM transplantation control (Figure 3.6C), indicating that TAM-supplied heparanase indeed plays a critical role in promoting tumor invasion. Interestingly, analysis of WT RT2 mice transplanted with *Hpa-Tg* BMDCs did not show an increase in tumor invasion over the WT BM control (Figure 3.6C), suggesting that the already high levels of heparanase in TAMs from WT RT2 tumors (Figure 3.5B) are sufficient to promote tumor invasion. This result also indicates that cancer cell-supplied heparanase (or heparanase derived from a minor non-BM derived stromal cell type) plays some role in enhancing invasion, as transplantation of *Hpa-Tg* BMDCs into WT RT2 tumors did not recapitulate the higher proportion of invasive tumors observed in the constitutive *Hpa-Tg* RT2 mice (Figure 3.3B). Therefore, heparanase promotes

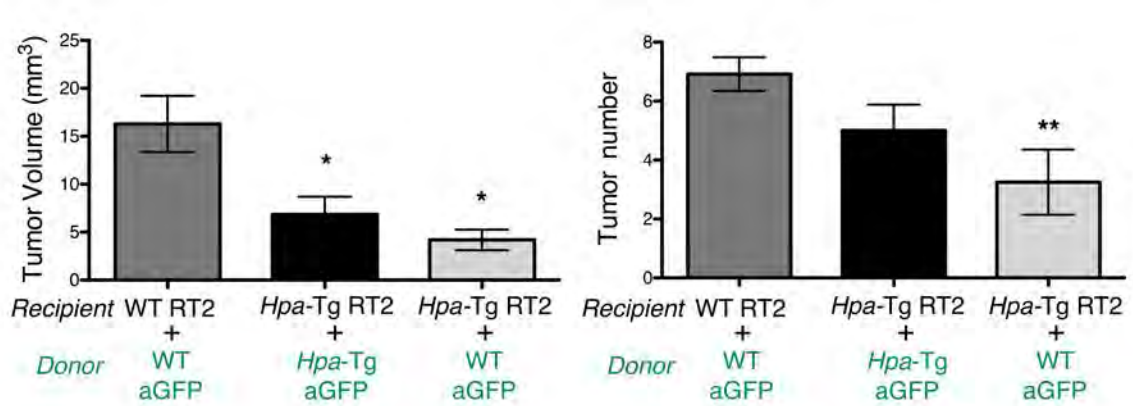


Figure 3.7. *Hpa-Tg* mice have increased sensitivity to irradiation and decreased tumor burden after BMT. Tumor volume and tumor number in lethally irradiated *Hpa-Tg* RT2 transplanted with either *Hpa-Tg* or *Hps^{-/-}* aGFP BM was found to be significantly decreased compared to WT RT2 mice transplanted with WT aGFP BM. (* $P < 0.05$, ** $P < 0.01$).

tumor invasion through both macrophage- and cancer cell-derived sources.

We also performed BM transplantation experiments in which *Hpa-Tg* RT2 mice were the transplant recipients. However, we found that several *Hpa-Tg* RT2 mice died within one week of irradiation, most likely due to intestinal inflammation. With treatment with antibiotics and a modified diet, a cohort of mice transplanted with either *Hpa-Tg* aGFP or WT aGFP BM was aged to 13.5 weeks. We found that both groups had significantly reduced tumor burdens (Figure 3.7), indicating that the tumors also exhibited an increased sensitivity to irradiation and these mice were excluded from any further analysis.

Heparanase deletion leads to increased tumor angiogenesis

As heparanase expression has been shown to enhance tumor angiogenesis (Vlodavsky et al., 2012), we investigated the effects of genetic manipulation of heparanase on blood vessel density in the RT2 model. Using the endothelial cell marker MECA32, we quantitated the total blood vessel area in tumor sections from WT RT2, *Hpa-Tg* RT2 and *Hpse*^{-/-} RT2 mice (Figure 3.8A). We found that while WT RT2 and *Hpa-Tg* RT2 mice had comparable tumor angiogenesis, *Hpse*^{-/-} RT2 mice had a 1.7-fold increase in vessel area (Figure 3.8B). We also investigated the pericyte coverage of the blood vessels as measured by the percent of the pericyte marker NG2 overlapping MECA32. We found that *Hpse*^{-/-} RT2 mice also exhibited a significant increase in pericyte coverage, with a 1.8-fold increase compared to WT RT2 and *Hpa-Tg* mice (Figure 3.8B).

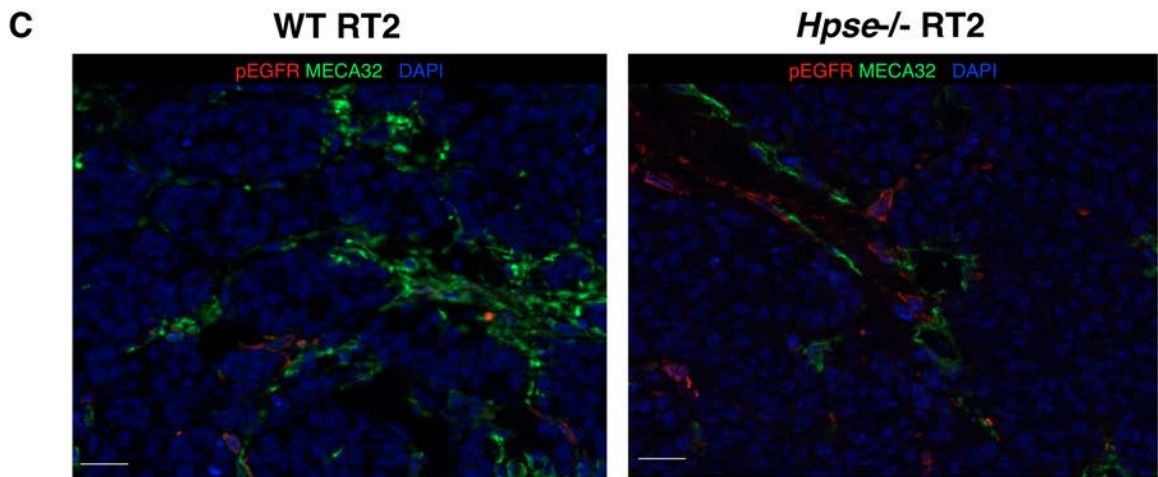
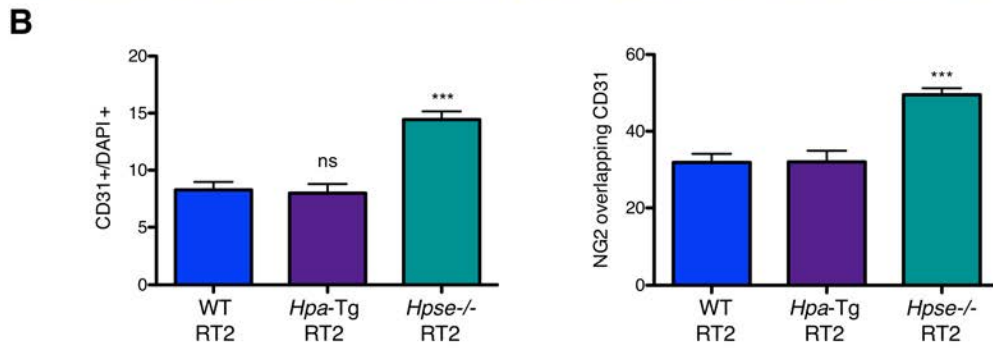
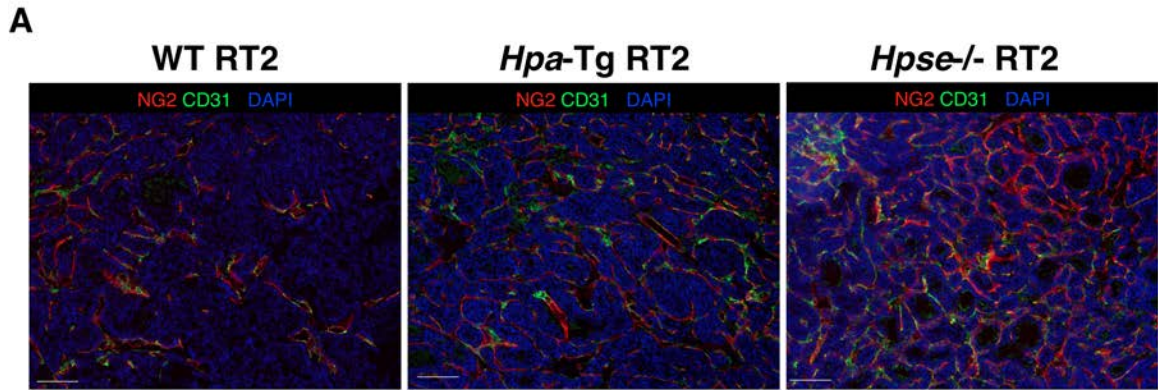


Figure 3.8. Heparanase knock-out leads to increased angiogenesis and pericyte coverage. (A) Representative images from tumors stained with CD31 (endothelial cells), NG2 (pericytes) and DAPI. Scale bar 100 μm . (B) Quantitation of the total CD31 area, normalized to DAPI area and the percentage of NG2 that is overlapping CD31 (pericyte coverage) using MetaMorph. (***) $P < 0.001$, ns= not significant). (C) Representative images of pEGFR staining in WT RT2 and *Hpse*^{-/-} RT2 tumors. Scale bar 20 μm .

The increased angiogenesis observed in the *Hpse*^{-/-} RT2 mice was unexpected, as heparanase has been described to play a pro-angiogenic role. However, given the increase in heparan sulfate levels along blood vessels in the *Hpse*^{-/-} RT2 mice, we hypothesized that this heparan sulfate was acting to sequester heparan sulfate-binding growth factors and thus enhancing angiogenesis. Previous work in the RT2 model has shown that the heparan binding epidermal growth factor HB-EGF is an important activator of EGFR signaling in pericytes, increasing pericyte coverage and supporting angiogenesis (Nolan-Stevaux et al., 2010). Therefore, we investigated whether activation of EGFR, as a read-out of HB-EGF binding, was increased in *Hpse*^{-/-} RT2 mice, to determine whether this was a potential explanation for the increased angiogenesis. Indeed, we saw increased pEGFR staining in tumors from *Hpse*^{-/-} RT2 mice, as compared to WT RT2 mice (Figure 3.8C). This staining was localized to cells adjacent to the MECA32⁺ endothelial cells, which is consistent with the localization of pericytes. Therefore, increased sequestration and activation of pericytes by HB-EGF is one potential explanation for the increased angiogenesis in *Hpse*^{-/-} RT2 mice.

Heparanase overexpression enhances peritumoral lymphangiogenesis

Given the roles we have identified for heparanase in promoting malignancy, we were interested in investigating whether other aspects of tumorigenesis were affected by manipulating heparanase levels. Examination of pancreatic tissue sections from *Hpa*-Tg RT2 mice revealed a significant increase in peritumoral lymphangiogenesis, visualized by staining with the lymphatic endothelial marker

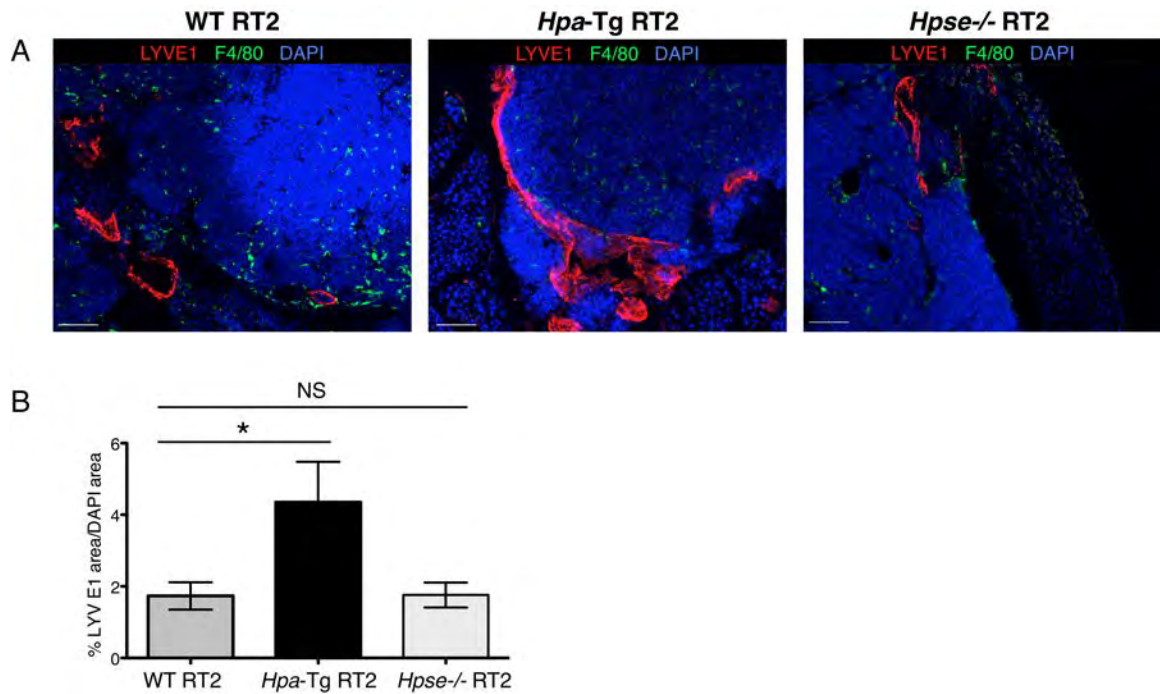


Figure 3.9. Enhanced peritumoral lymphangiogenesis in *Hpa-Tg* RT2 mice. (A) Representative images depicting increased lymphangiogenesis in *Hpa-Tg* mice, compared to WT RT2 and *Hpse*^{-/-} RT2. 35 μ m frozen sections were stained for LYVE-1 (red), F4/80 (green) and DAPI (blue). Scale bar 100 μ m. (B) Lymphangiogenesis was quantitated in an area 500 μ m in peritumoral diameter using MetaMorph software. Total LYVE-1+ area was divided by total DAPI+ area. *Hpa-Tg* RT2 mice had significantly increased lymphangiogenesis compared to WT RT2 mice; * $P=0.039$, NS= not significant. WT RT2 and *Hpa-Tg* RT2, $n=12$ mice; *Hpse*^{-/-} RT2, $n=6$ mice.

LYVE-1 (Figure 3.9A). Co-staining with the macrophage marker F4/80 confirmed that these were lymphatic vessels and not LYVE-1⁺ macrophages. Quantitation of peritumoral lymphangiogenesis revealed a two-fold increase in the *Hpa-Tg* RT2 mice compared to WT RT2 mice (Figure 3.9B). Analysis of *Hpse*^{-/-} RT2 mice showed a comparable amount of lymphangiogenesis to WT RT2 mice, indicating that while heparanase overexpression induces additional lymphangiogenesis, it is not required for the basal level of peritumoral lymphangiogenesis seen in WT mice.

Growth factor expression is not affected by heparanase modulation

We have shown that heparanase modulation plays roles in angiogenesis and lymphangiogenesis, however this could be due to increased growth factor release from the matrix by heparanase, or could be due to increased expression of growth factors, as has been previously reported (Vlodavsky et al., 2012). To determine if growth factor expression was altered with genetic modulation of heparanase, RNA was isolated from whole tumors from WT RT2, *Hpa-Tg* RT2 and *Hpse*^{-/-} RT2 mice and expression of *VEGF-A*, *VEGF-C*, *VEGF-D*, *FGF-2* and *HGF* were analyzed. We found that there were no significant differences between the genotypes for all of these factors (Figure 3.10). We also investigated whether there were any differences in each specific cell type that was being masked in the bulk tumor analysis. Therefore we examined the expression of *VEGF-A*, *VEGF-C*, *VEGF-D* and *FGF-2* in sorted cell populations shown in Figure 3.5A. We found that each of these genes had varying expression patterns,

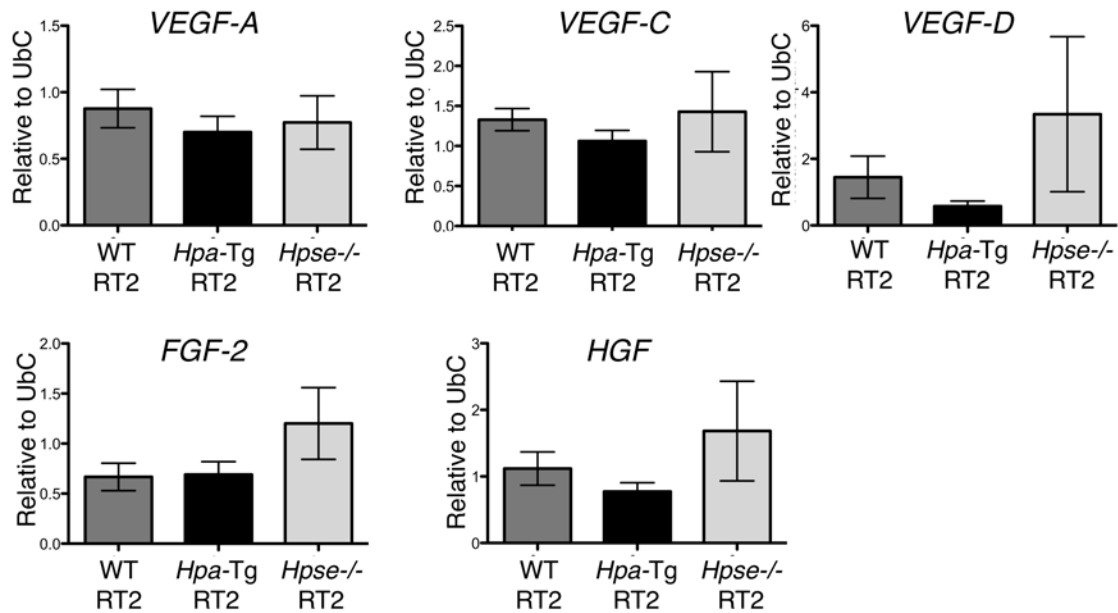


Figure 3.10. Lymphangiogenic growth factors are not upregulated in tumors. RNA was isolated from whole tumors from WT RT2, *Hpa-Tg* RT2 and *Hpse-/-* RT2 mice and qPCR was performed for *VEGF-A*, *VEGF-C*, *VEGF-D*, *FGF-2* and *HGF*. Gene expression was normalized to *UbC*. No significant differences were seen between any of the genotypes.

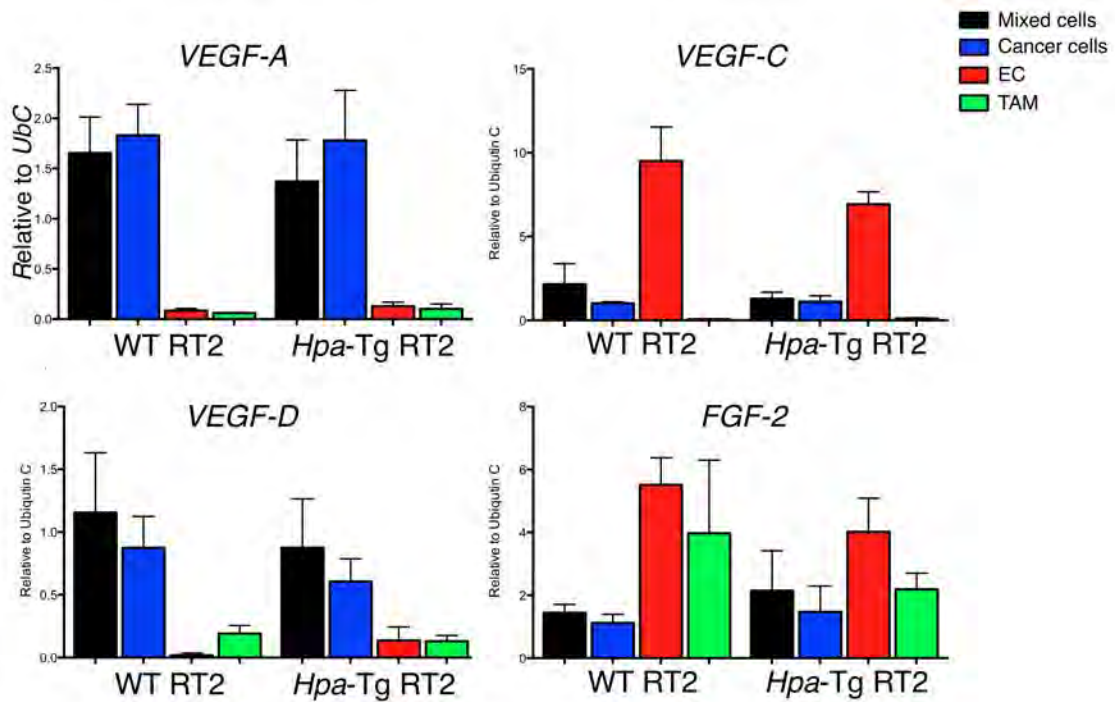


Figure 3.11. Lymphangiogenic growth factors are not upregulated in cancer cells, endothelial cells and TAMs. Expression of lymphangiogenic growth factors was performed on sorted cell populations described in Figure 3.5. No significant differences in expression were seen for any growth factors. $n=4$ independent experiments.

however we observed no significant differences between WT RT2 and *Hpa-Tg* RT2 mice (Figure 3.11). Therefore, consistent with the importance of heparanase in releasing ECM-tethered growth factors (Vlodavsky et al., 2012), it is likely that cleavage of HSPGs by heparanase leads to increased bioactive growth factors.

Heparanase overexpression enhances formation of LEC-like structures

Myeloid cells have been shown to play important roles in lymphangiogenesis, through secretion of pro-lymphangiogenic growth factors or by direct incorporation into lymphatic vessels (Zumsteg and Christofori, 2012). Given the high levels of heparanase expression in TAMs, we were therefore interested in investigating the impact of heparanase overexpression in macrophages in the context of lymphangiogenesis. Previous work has shown that macrophages can be induced to trans-differentiate into lymphatic endothelial-like cells (Maruyama et al., 2005; Zumsteg et al., 2009), and we thus sought to determine whether heparanase overexpression could enhance this process.

Bone marrow was isolated from WT or *Hpa-Tg* mice and differentiated into bone marrow-derived macrophages (BMDMs) in culture using CSF-1. These cells were then plated on a mixture of Matrigel and lymphatic endothelial cell (LEC) media and incubated for up to 8 days (Figure 3.12A). As shown previously (Maruyama et al., 2005), macrophages clustered together and formed LEC-like structures. Interestingly, *Hpa-Tg* BMDM showed an increased number and size of these structures at the end of the assay (Figure 3.12B). These structures were

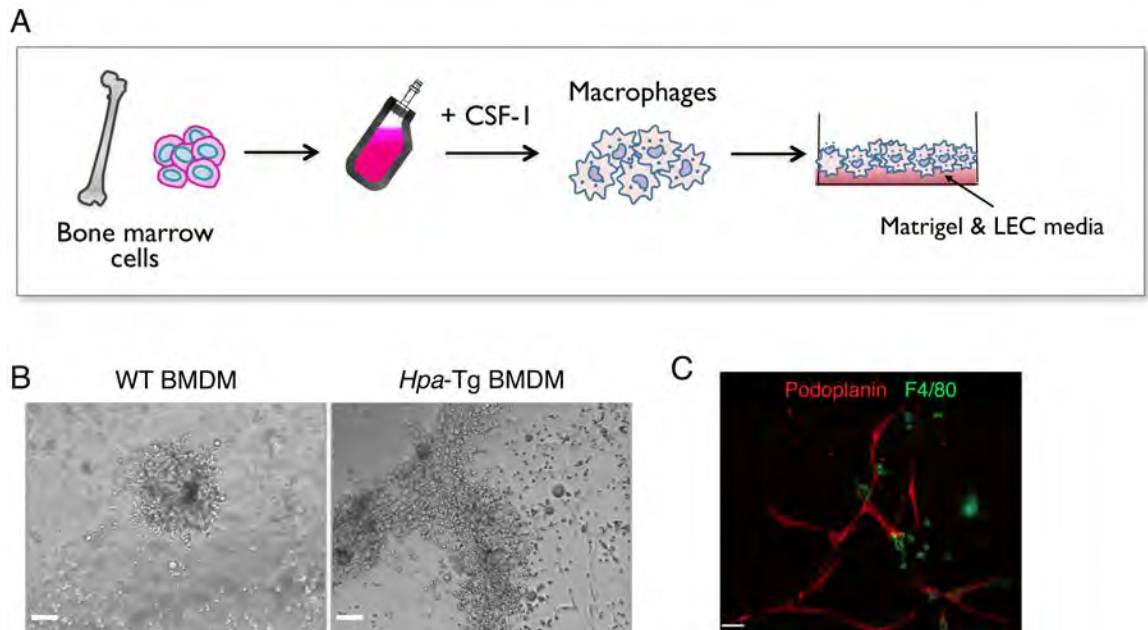


Figure 3.12. *Hpa-Tg* macrophages show increased trans-differentiation into lymphatic-like structures. (A) Schematic of experimental design. (B) Representative day 8 cultures of BMDM plated on Matrigel and EGM-2. Scale bar 100 μm . (C) Representative immunofluorescence staining for podoplanin and F4/80 on day 8 *Hpa-Tg* cultures. Scale bar 100 μm .

also confirmed to express the LEC marker podoplanin and no longer express the macrophage marker F4/80 (Figure 3.12C). To further characterize these structures, we isolated RNA from cells at either the establishment of the cultures or after eight days of culture when mature structures have formed. We saw no significant difference in any marker at day 0 between WT and *Hpa-Tg* BMDM (Figure 3.13). As expected, the *Hpa-Tg* cultures at day 8 trended towards increased expression of the LEC markers *LYVE-1*, *podoplanin*, and *VEGFR-3* (Figure 3.13). We saw a concordant decrease in *VEGFR-1* and *VEGFR-2* at day 8.

We found that there was a significant increase in the expression of the growth factors *VEGF-C*, *VEGF-D*, and *FGF-2*, which have all been shown to be pro-lymphangiogenic (Tammela and Alitalo, 2010) (Figure 3.13). However, there was no increase in *VEGF-A* or *HGF* mRNA expression, which have also been reported to promote lymphangiogenesis (Tammela and Alitalo, 2010). To test whether these growth factors were able to increase lymphatic structure formation, individual recombinant proteins were added to the media during the assay, and the total number of structures was counted at day 8. *VEGF-C* and *FGF-2* increased the number of structures formed in the WT condition, to levels seen with *Hpa-Tg* BMDM (Figure 3.14), with somewhat less pronounced increases for *VEGF-A* and *HGF*. However, there was no further increase in structure formation when these factors were added to *Hpa-Tg* cells, indicating they are already at sufficiently high levels in this experimental condition.

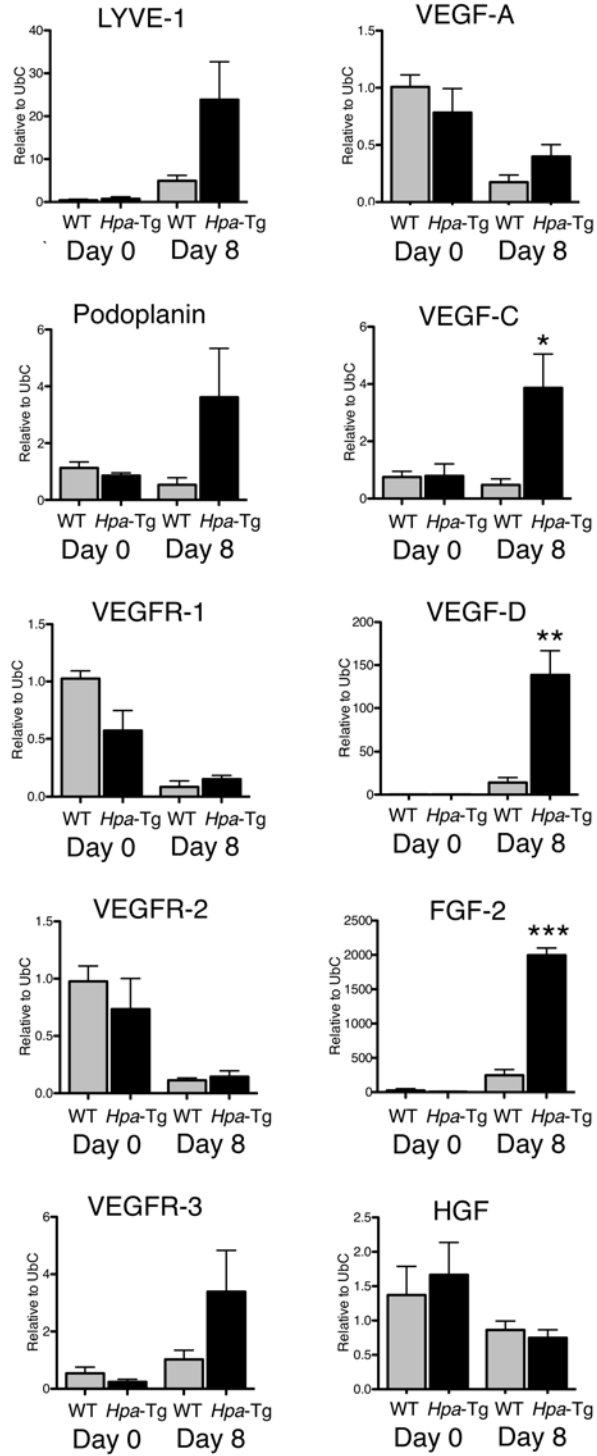


Figure 3.13. Upregulation of LEC-related genes in *Hpa*-Tg cultures. qPCR analysis of day 0 and day 8 cultures. mRNA was isolated from cells plated in 24-well dishes and expression analysis determined for the genes listed, relative to ubiquitin C. At day 8 *Hpa*-Tg cultures showed a significant upregulation of VEGF-C (* $P=0.029$), VEGF-D (** $P=0.005$) and FGF-2 (***) $P<0.0001$). $n=4$ independent experiments.

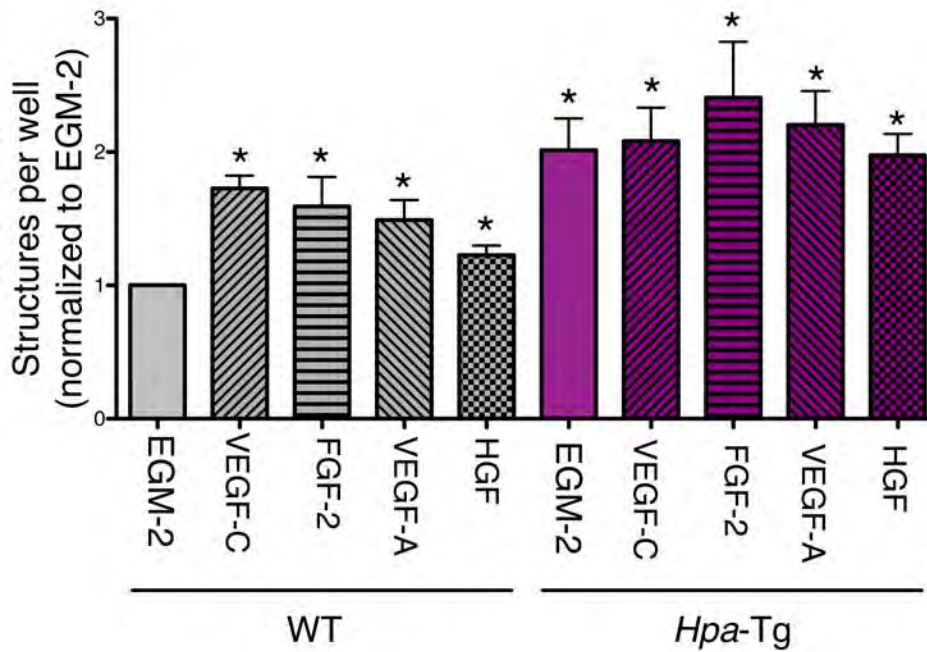


Figure 3.14. Growth factor addition enhances the formation of LEC-like structures in WT cultures. Growth factors were added to cultures and the number of lymphatic endothelial cell-like structures were counted at day 8 and normalized to the WT EGM-2 condition for each experiment ($n=3-4$ repeats per growth factor). The source of cells (WT or *Hpa-Tg*) is indicated below. * $P<0.05$ compared to WT EGM-2 using Mann-Whitney test.

Therefore, heparanase overexpression increases the ability of BMDM to form LEC-like structures in a process that may be due to their increased production/enhanced bioavailability of pro-lymphangiogenic growth factors.

Discussion

Heparanase expression promotes tumorigenesis in PanNETs

PanNETs are a clinically challenging tumor type, due to their marked disease heterogeneity and limited understanding of the molecular basis for their development. Through our collaboration with Dr. Laura Tang in MSKCC's Pathology department, we are uniquely situated to identify factors that may be important for tumorigenesis in a large sample set from patients with PanNETs. We have found that while heparanase is expressed at very low levels in normal islets, its expression is increased 40-fold in primary tumors and metastatic tumors, and we see that increased heparanase levels are significantly correlated with increased malignancy and the presence of metastatic disease. Our results identify heparanase as a potential novel prognostic indicator and as an intriguing therapeutic target for PanNETs.

As we have validated the relevance of heparanase in PanNET patient samples, we sought to investigate the molecular mechanisms by which heparanase promotes tumorigenesis. We turned to the well-characterized RT2 model of pancreatic islet carcinoma to investigate the specific roles of heparanase in tumor progression. Previous work has shown that heparanase is upregulated

during the course of tumorigenesis in RT2 mice and treatment with a heparan sulfate mimetic has indirectly implicated heparanase and heparan sulfate-mediated signaling in tumorigenesis (Joyce et al., 2005), however the specific roles of the heparanase enzyme itself were unknown. Utilization of *Hpa-Tg* mice, which overexpresses heparanase, and *Hpse*^{-/-} mice, which have deletion of heparanase, allowed us to interrogate the roles of heparanase modulation in a spontaneous mouse model of cancer for the first time.

Heparanase promotes invasion through cancer cell and TAM sources

While heparanase has been described to increase cancer invasion in cell lines (Arvatz et al., 2011), here we show that heparanase expression strikingly enhances tumor invasion in a spontaneous tumor model. We find that overexpression of heparanase leads to a 2.5 fold increase in the most invasive class of tumors and that deletion of heparanase leads to a significant decrease in tumor invasion. We propose that the increase in tumor invasion modulated by heparanase is at least partially a result of extracellular matrix degradation, demonstrated by the decreased heparan sulfate levels at the tumor invasive front of WT RT2 mice. Consistently, the overall decrease in heparan sulfate levels in the *Hpa-Tg* RT2 tumors and the increased levels in the *Hpse*^{-/-} RT2 tumors demonstrates the activity of heparanase in heparan sulfate remodeling.

Given the correlation between increased heparanase expression levels and metastasis in PanNET and other tumor types, we were interested in whether

heparanase expression increases metastasis in the RT2 model. The RT2 model has limited utility in studying metastasis, as the mice typically die due to the hypoglycemia as a result of their primary tumors before extensive metastasis has occurred. Our analysis found no difference between the genotypes in local lymph node metastasis at 13.5 weeks, however when looking at the distant metastatic site of the liver at 16 weeks of age, we saw a trend towards increased metastasis in the *Hpa-Tg* mice. This is consistent with our data in PanNET patients, however this trend remains to be further validated to make definitive conclusions about the role of heparanase in metastasis in RT2 tumorigenesis.

As we are interested in studying the specific roles of the many cell types within the tumor microenvironment, we investigated which cells were the sources of heparanase. Cell sorting in WT RT2 mice revealed that heparanase is expressed by cancer cells and to a greater extent by TAMs. This was intriguing as previous analysis of macrophage density in human PanNET samples revealed a significant, positive correlation with poor prognosis and metastasis, implicating TAMs in PanNET tumorigenesis (Pyonteck et al., 2012), similar to our results with heparanase. Additionally, studies in the RT2 model have shown that TAM-supplied cysteine cathepsins play critical roles in tumorigenesis (Gocheva et al., 2010), leading us to question whether TAM-supplied heparanase was similarly important for promoting tumor invasion.

Using BM transplantation studies, we found TAM-supplied heparanase promotes invasion, as removal of heparanase from BMDCs does indeed significantly impair tumor invasion. Interestingly, we saw that transplantation of *Hpa-Tg* BM into WT RT2 mice was not sufficient to increase invasion to the levels seen in the constitutive *Hpa-Tg* mice, also implicating a non-BMDC population in invasion. We hypothesize that these cells are cancer cells, as they make up the majority of the tumor bulk, however it is also possible that heparanase supplied by another non-BM derived stromal cell type could also be influencing tumor invasion. The functional importance of these cells is very unlikely, as they represent a relatively small source of heparanase that would be masked by high levels of heparanase produced by the cancer cells. Therefore, we conclude that heparanase promotes tumor invasion through both TAM-derived and cancer cell-derived sources.

We were interested in testing the importance of heparanase overexpression in cancer cells while modulating TAM heparanase levels; however, during the course of the BM transplantation studies, we were surprised to discover that *Hpa-Tg* RT2 mice have an increased sensitivity to irradiation, with increased morbidity apparently due to intestinal inflammation and significantly lower tumor burdens. This increased sensitivity is consistent with a previous report in which heparanase promotes a chronic inflammation circuit in the intestines of *Hpa-Tg* mice, amplifying inflammatory conditions (Lerner et al., 2011). Due to these unexpected experimental complications, we omitted any further investigation of the transplanted *Hpa-Tg* RT2 mice.

Heparanase plays pleiotropic roles in the tumor microenvironment

Interestingly, we found that genetic modulation of heparanase levels had differential effects on blood vessel and lymphatic vessels, whereas the literature has ascribed positive roles for heparanase in both of these processes. While *Hpa-Tg* RT2 mice exhibited increased peritumoral lymphangiogenesis, *Hpse*^{-/-} RT2 mice exhibited increased tumor angiogenesis. Analysis of growth factors involved in these processes revealed no differences in mRNA expression levels, implicating the role of heparanase in growth factor release. The opposing phenotypes seen in these mice underscore the complexity of matrix remodeling and homeostasis. The balance of growth factor release and bioavailability by heparanase overexpression can thus be countered by heparan sulfate accumulation and potential increases in heparan sulfate signaling.

Heparanase has been implicated in promoting angiogenesis, through release of pro-angiogenic growth factors such as VEGF-A (Vlodavsky et al., 2012). Surprisingly, we found no increase in angiogenesis in *Hpa-Tg* RT2 mice, but rather an increase in *Hpse*^{-/-} RT2 mice. In the RT2 model, cancer cells produce high levels of VEGF and thus VEGF signaling may be saturated, with any increase in the bioavailability of VEGF by heparanase having a negligible effect. However, the increased accumulation of heparan sulfate along the vessels in *Hpse*^{-/-} RT2 mice raised the interesting possibility that it was acting as a sink for heparan binding growth factors and thus activating the vasculature. Previous

work in the RT2 model showed that one such factor, HB-EGF, plays an important role in activating pEGFR on pericytes, leading to increased pericyte coverage and support of angiogenesis (Nolan-Stevaux et al., 2010). Consistent with this, we saw increased pEGFR staining in *Hpse*^{-/-} RT2 mice and a significant increase in pericyte coverage.

The striking increase in lymphangiogenesis observed in the *Hpa*-Tg RT2 mice was intriguing, as a previous study in head and neck cancer showed that heparanase expression correlated with lymphatic vessel density in patient samples (Cohen-Kaplan et al., 2008). It has also been shown that heparanase overexpression in cell lines can lead to an upregulation of VEGF-C (Cohen-Kaplan et al., 2008); however, we found that expression of pro-lymphangiogenic growth factors was not increased in *Hpa*-Tg RT2 mice, implicating increased bioavailability of VEGF-C, or another pro-lymphangiogenic growth factor, in promoting lymphangiogenesis. Consistently, overexpression of VEGF-C in a β -cell-specific manner led to increased peritumoral lymphangiogenesis in the RT2 model (Mandriota et al., 2001).

In addition to the proposed release of VEGF-C leading to increased lymphangiogenesis, we investigated the role of myeloid cells in this process, given their importance in lymphangiogenesis (Zumsteg and Christofori, 2012). We found that heparanase overexpression enhanced the ability of macrophages to trans-differentiate into LEC-like structures. This trans-differentiation was

accompanied by increased expression of lymphangiogenic markers and pro-lymphangiogenic growth factors. This increased expression could be due to the increased expression by trans-differentiated cells, of which there are more of in *Hpa-Tg* cultures, or heparanase could in fact be driving this trans-differentiation. To begin to interrogate this, we added growth factors to the media of cultures, and found that this was able to increase the number of LEC-like structures in WT cultures to similar levels seen in the *Hpa-Tg* group. However, growth factor addition did not further increase the number of structures in the *Hpa-Tg* group, indicating that growth factor levels or signaling were at sufficiently high levels in this experimental condition. Our results are consistent with a model in which heparanase overexpression leads to increased release and bioavailability of VEGF-C, activating lymphangiogenesis. In addition, myeloid cells that overexpress heparanase can help to support this lymphangiogenesis, either through direct incorporation into lymphatic vessels as has been shown in previous studies (Zumsteg et al., 2009), or by increased production of pro-lymphangiogenic growth factors. Given the controversial nature of myeloid incorporation into lymphatic vessels, we had hoped to use our BM transplantation studies to address this question. However, due to the radiosensitivity of the *Hpa-Tg* mice, unfortunately these experiments were not possible.

In conclusion, our studies have revealed multiple novel functions for heparanase in enhancing pancreatic neuroendocrine tumorigenesis. Using complementary genetic approaches, we found that heparanase overexpression induces

lymphangiogenesis and promotes trans-differentiation of macrophages into LEC-like structures. Counterintuitively, deletion of heparanase increases tumor angiogenesis in RT2 mice, thus highlighting the complexity of the roles that matrix-remodeling enzymes play. Additionally, we showed that heparanase produced by both TAMs and cancer cells is important in promoting tumor invasion. Our results from the RT2 model are especially relevant, as we have also shown that heparanase expression significantly correlates with increased malignancy in patients with PanNETs. Therefore, heparanase represents an attractive therapeutic target and a potential prognostic factor for PanNET patients.

CHAPTER FOUR

Characterization and Development of a Mouse Model of Poorly Differentiated PanNETs

PanNETs are a rare tumor type, but pose major clinical challenges that arise in part from marked disease heterogeneity and varied patient outcome (Halfdanarson et al., 2008; Kulke et al., 2011). One of the most important issues is to accurately stratify patients into prognostic groups that could provide critical benefits in clinical management of the disease. Currently, it is known that patients with metastatic disease have poor prognosis and that patients with poorly differentiated PanNETs have the worst prognosis (Yao et al., 2008). As described in Chapter 3, our results have indicated that the matrix remodeling enzyme heparanase is a novel indicator of poor patient prognosis in well-differentiated PanNETs, and high heparanase expression is correlated with metastatic disease. However, very little is known about poorly differentiated PanNETs (PD-PanNETs), both in the pathology of the disease and their treatment response (Davies and Conlon, 2009).

In this study we have identified and characterized a previously undescribed class of poorly differentiated PanNETs in the RT2 model. We have established the tools to investigate the development and molecular mechanisms driving this tumor type *in vivo*. In parallel, we have initiated the development of a mouse model for PD-PanNETs to use in preclinical testing, as none currently exists.

Results

Identification of a novel class of invasive, poorly differentiated tumors

During the course of our analysis of lymph node metastases in serially sectioned pancreata from RT2 mice, we identified a previously undescribed class of tumors. These tumors were found due to their loss of insulin expression (Figure 4.1A). In addition, these tumors were highly invasive and anaplastic, leading us to term these tumors poorly differentiated invasive carcinomas (PDIC).

Discovery of a set of tumors that had lost insulin expression was surprising, as it had been previously thought that all RT2 tumors expressed insulin at very high levels due to their origin from β -cells. By H&E staining the PDICs appeared similar to the insulinomas, however there remained the possibility that these arose from a different cell of origin. To determine whether they were still driven by the SV40 T-antigen oncogene, we stained sections with a T-antigen antibody, and found that all tumors expressed T-antigen, including tumors that had lost insulin expression (Figure 4.1B).

PDICs exhibit a high mitotic index

High-grade PanNETs are characterized by their high mitotic index (Reidy et al., 2009). Therefore, we were interested in whether these PDICs also exhibited an increased mitotic index. As depicted in Figure 4.2, PDICs that have lost insulin

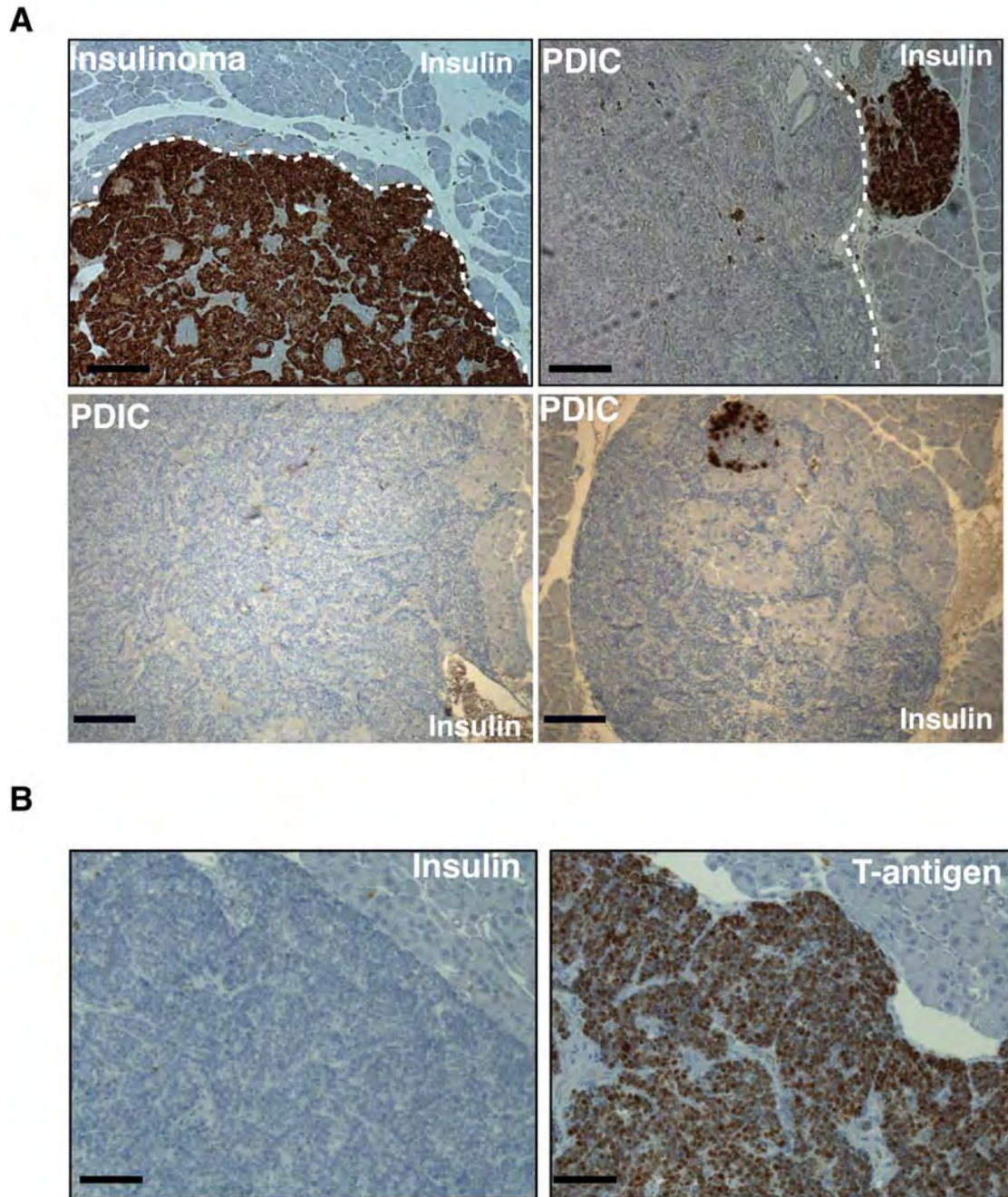


Figure 4.1. Identification of PDICs. (A) IHC for insulin was performed on paraffin sections from RT2 mice. While the majority of the tumors produce high levels of insulin, PDICs are negative for insulin staining. (B) Adjacent sections were stained for insulin and T-antigen. PDICs remained positive for T-antigen staining. Scale bar 50 μ m.

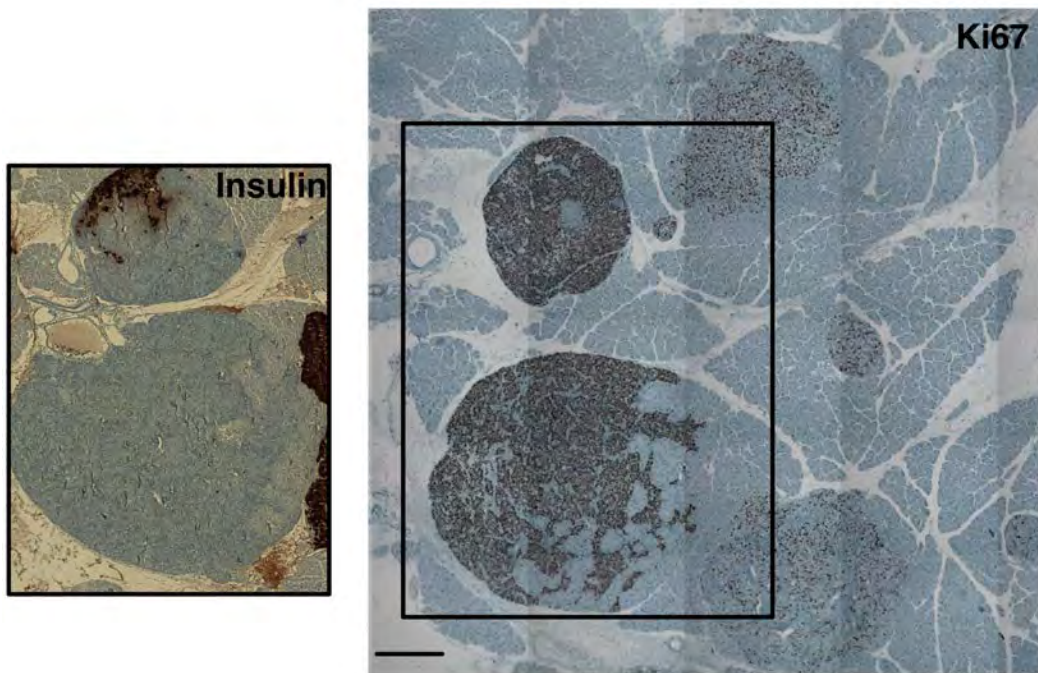


Figure 4.2. PDICs exhibit a high mitotic index. Adjacent tumor sections were stained for insulin and Ki67. PDICs that do not express insulin were found to have a very large proportion of Ki67+ proliferating cells. Scale bar 200 μ m.

(shown in the inset), have a markedly higher proportion of cells that are Ki67 positive, as compared to tumors that maintain insulin expression, depicted on the right side of the image. Therefore, PDICs in the RT2 model are highly proliferative, similar to poorly differentiated, high-grade PanNET tumors in patients.

PDICs occur in the majority of RT2 mice

PDICs have not been previously described before in the RT2 model and it was unknown whether these tumors were rare or were present in all mice but had been previously missed. To thoroughly investigate the frequency of PDICs, we completely sectioned through the entire pancreas of RT2 mice and examined every 10th slide to ensure that each tumor throughout the tissue was represented and analyzed. When staining for insulin, we found that while all mice had seven to ten insulinomas, 70% of WT RT2 mice examined also had at least one PDIC. Additionally, through our investigation of metastasis in *Hpa-Tg* RT2 and *Hpse*^{-/-} RT2 mice, we also found that PDICs were present in approximately 60% of these mice as well, indicating heparanase expression has no impact on the presence of PDICs. However, our analysis has revealed that PDICs are more common than expected, constituting approximately 10% of all tumors.

PDICs exhibit loss of neuroendocrine markers

Given the loss of insulin expression in PDICs, we next investigated whether other markers of β -cells and neuroendocrine cells were also absent in these tumors. Tissues containing both PDICs and insulinomas were stained for a panel of cell type-specific markers (Klimstra et al., 2010; Oliver-Krasinski and Stoffers, 2008). Synaptophysin, a marker of neuroendocrine cells, was found to be generally expressed in both insulinomas and PDICs, however it exhibited heterogenous downregulation in some PDICs (Figure 4.3). An additional neuroendocrine marker, chromogranin A, was found to be completely absent in PDICs. Additionally, the transcription factors MafA, Nkx 6.1 and Pdx1 were also absent in PDICs (Figure 4.3). Therefore, PDICs exhibit loss of multiple markers of neuroendocrine differentiation.

As PDICs have lost all markers of β -cells, it raised the possibility that they are tumors that have arisen from one of the other neuroendocrine cell types that constitute pancreatic islets. While β -cells represent the major cell type in islets, alpha-cells and delta-cells are also present, and tumors such as glucagonomas and somatostatomas can arise from these cells (Davies and Conlon, 2009). Also, it has been previously shown that under extreme β -cell loss, alpha-cells can be converted into β -cells (Thorel et al., 2010), indicating that there is plasticity between the different neuroendocrine cell types of the islets. Therefore, there is also the possibility that these tumors could reflect the converse situation, in which

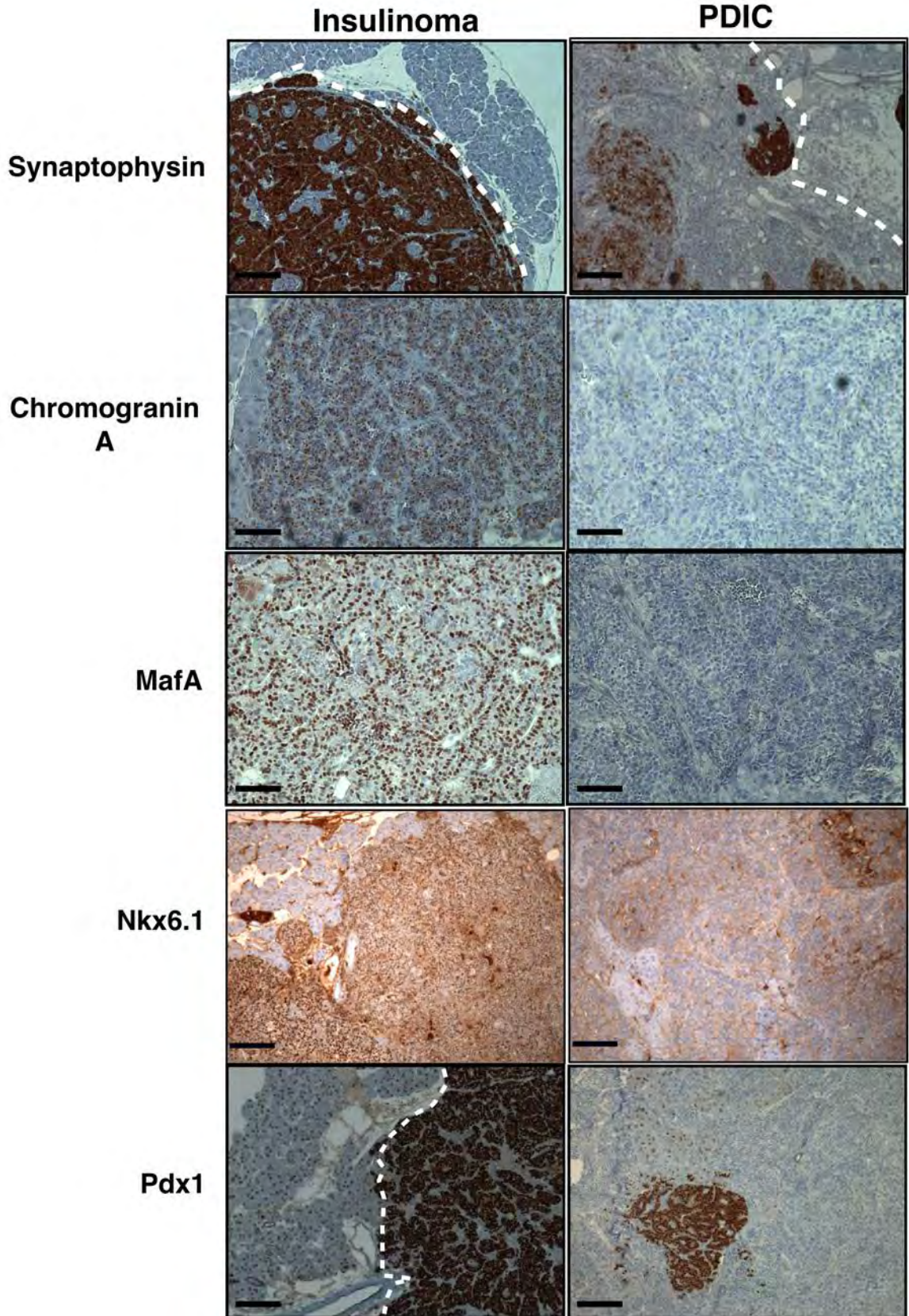


Figure 4.3. PDICs exhibit loss of multiple neuroendocrine markers. Sections were stained for the following markers of neuroendocrine differentiation: Synaptophysin, Chromogranin A, Maf A, Nkx2.1 and Pdx1. While insulinomas all stained positive for these markers, PDICs exhibited loss of these markers. Scale bar 50 μ m.

β -tumor cells transdifferentiate into one of the other pancreatic neuroendocrine cell types. We stained tissue sections for glucagon, a marker of alpha-cells, and somatostatin, a marker of delta-cells. We saw that normal islets exhibited a small proportion of cells that stained positive for these cell markers, which were also seen with less frequency in tumors, as they were crowded out by the tumor cells. However, we saw that there was no staining of PDIC or insulinoma tumor cells (Figure 4.4), indicating that PDICs do not express markers of any pancreatic neuroendocrine cell type.

PDICs specifically express Id1

Characterization of PDICs has revealed that they have lost multiple markers of β -cell differentiation, however, factors that were specifically expressed by these tumors remained unknown. We therefore undertook a candidate-based approach to determine a specific, positive marker of PDICs. Due to the apparent dedifferentiation of these tumors, we investigated the expression pattern of Id1, one of the inhibitor of DNA binding (Id) proteins. Id1 has been shown to inhibit differentiation, to stimulate proliferation and to be expressed by embryonic stem cells, adult stem cells and cancer stem cells (Barrett et al., 2012; Nam and Benezra, 2009; Perk et al., 2005).

We stained tissue sections from RT2 mice and found that Id1 stained all endothelial cells, which was expected as Id1 has been described previously to play an important role in angiogenesis (Lyden et al., 1999). Tumor cells in

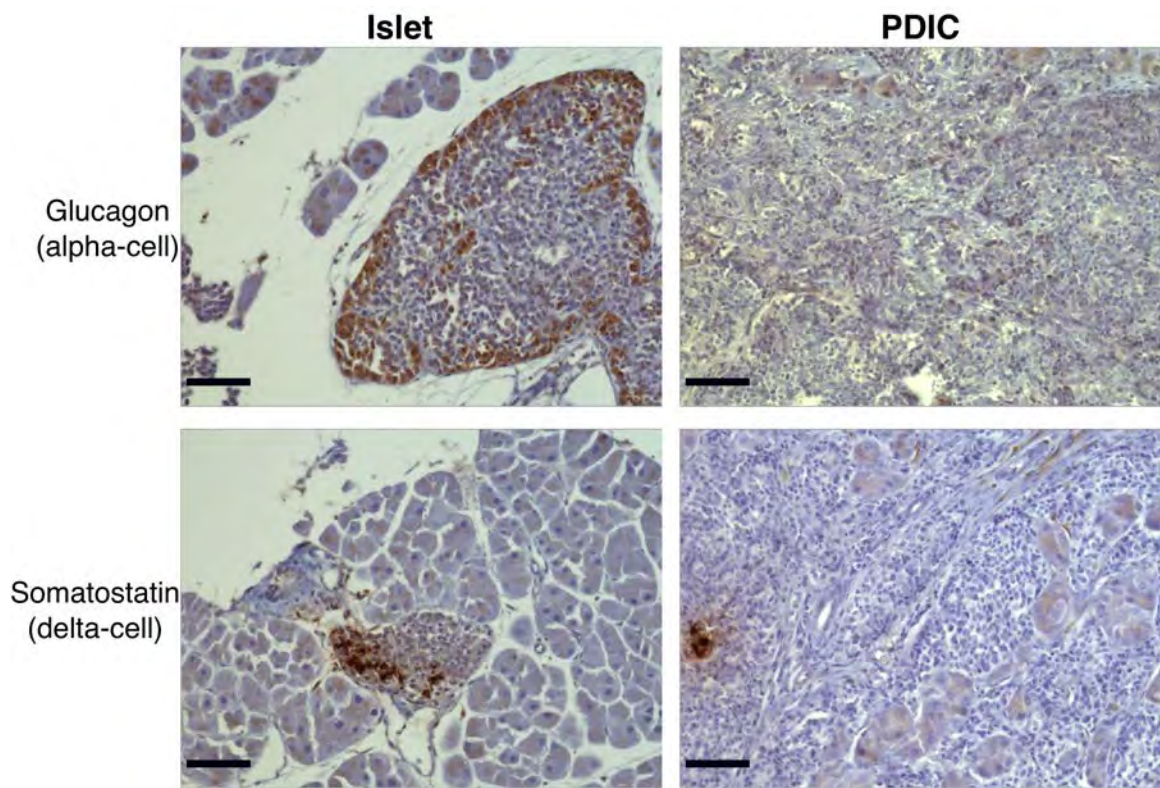


Figure 4.4. PDICs do not express alpha-cell or delta-cell markers. Tissues were stained for glucagon, to mark alpha-cells, and somatostatin, to mark delta-cells. PDICs were negative for these markers. Scale bar 50 μ m.

insulinomas had no detectable Id1 staining (Figure 4.5A). Strikingly, we found that PDICs specifically stained for Id1, exhibiting a nuclear staining pattern (Figure 4.5A). Through staining each of the PDICs that had been previously identified by their loss of insulin, we determined that all PDICs were positive for Id1 and that Id1 staining was mutually exclusive from insulin staining. While most of the PDIC tumors were found to be entirely positive for Id1, we found several instances in which Id1 was expressed only in tumor cells along the invasive front of the tumor (Figure 4.5B). We also observed several tumors in which Id1 staining was found in the exocrine cells directly adjacent to a PDIC, while we never saw exocrine Id1 staining in any other instance (Figure 4.5C). We found that PDICs specifically were also positive for Id3 (Figure 4.6), another Id family member which can play a redundant role to Id1 (Perk et al., 2005).

We also confirmed the expression of Id1 in protein lysates from a panel of RT2 tumors. Most tumors showed moderate levels of Id1, most likely originating from the Id1 produced by endothelial cells within the vasculature of the tumor. Interestingly, one tumor showed much higher levels of Id1 (Figure 4.7, lane #5). Consistent with the immunohistochemistry staining of the PDICs, we saw that this tumor had corresponding absences of insulin and MafA (Figure 4.7).

Given the described roles of Id1 in cell differentiation, we were interested in whether the expression of Id1 by PDICs was what was driving their loss of differentiation, or rather was a marker of their poorly differentiated state. To

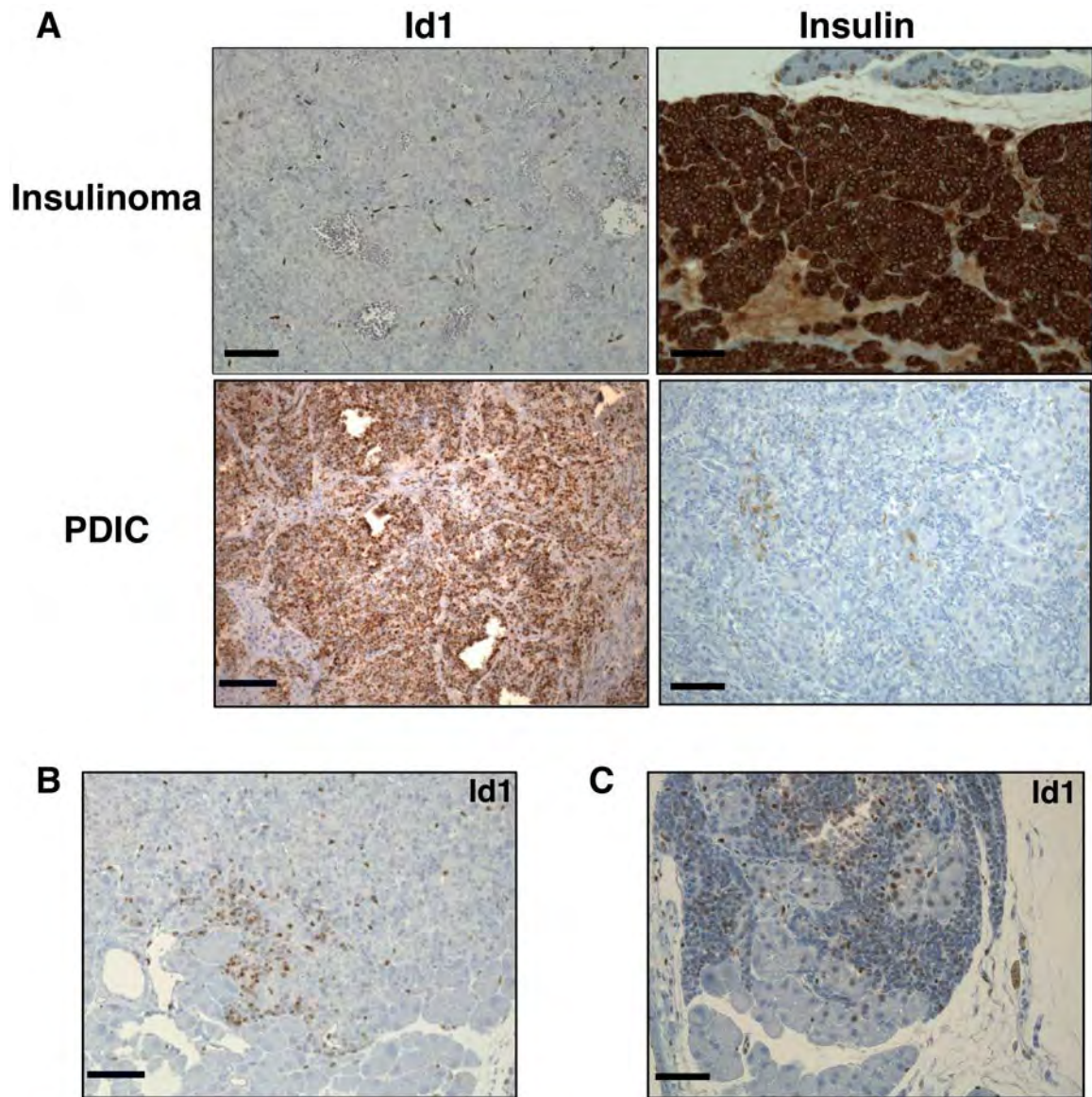


Figure 4.5. Id1 is expressed by PDICs. (A) Adjacent sections were stained for Id1 and insulin. PDIC tumor cells specifically expressed Id1, while insulinomas did not, with the only staining present in endothelial cells. (B) Id1⁺ cells (brown) are evident at the invasive front of a tumor. (C) Id1 staining is observed in exocrine cells adjacent to a PDIC. Scale bar 50 μ m.

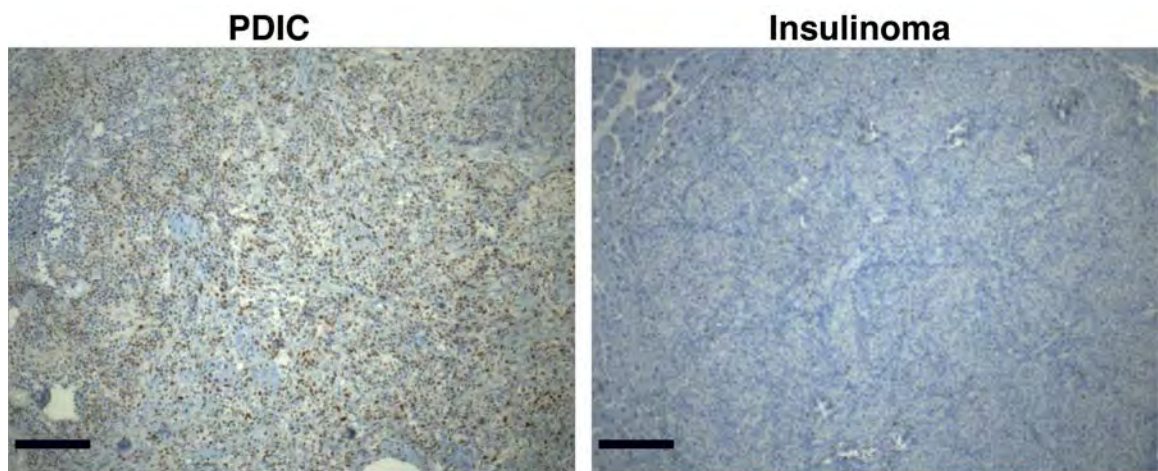


Figure 4.6. Id3 is expressed by PDICs. IHC staining for Id3 showed this protein is specifically expressed in PDICs, and not insulinomas. Scale bar 50 μ m.

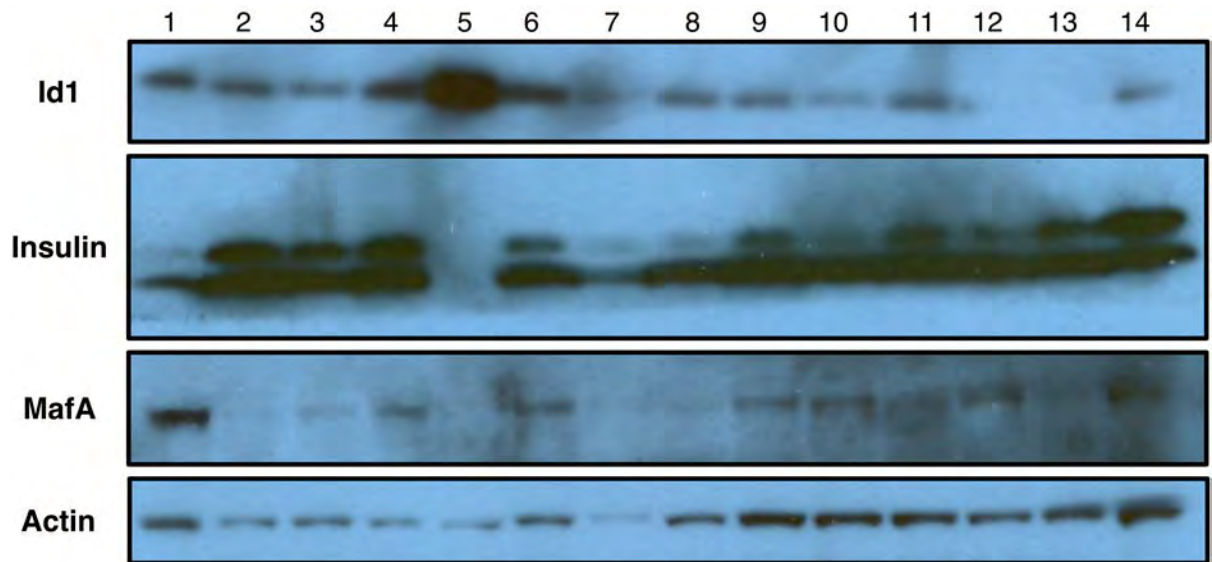


Figure 4.7. Western blots of RT2 tumors. A panel of RT2 tumor lysates were blotted for Id1, insulin, MafA and actin as a loading control. The 5th tumor lysate is a PDIC, as it has high Id1, and absent insulin and MafA.

investigate the role of Id1, we overexpressed Id1 in a tumor cell line derived from an RT2 tumor. The increased expression of Id1 was confirmed by qPCR for Id1 (Figure 4.8A). We then performed qPCR for the genes for synaptophysin (*Syp*), insulin (*Ins2*), *MafA*, and Neurog3 (*Ngn3*), another transcription factor involved in β -cell differentiation, and found that there was no difference in the expression of each of these genes upon overexpression of Id1 (Figure 4.8B). Therefore, these data indicate that Id1 expression is not sufficient to induce dedifferentiation of an RT2 tumor cell line.

Development of mouse models to study PD-PanNETs

As the cell of origin and pathogenesis of PD-PanNETs is unknown, we sought to develop tools that would allow us to address this critically important question. The identification of Id1 as being specifically expressed in PDICs but not in insulinomas allows us to use Id1 expression in tumor cells as a surrogate marker for PDICs. We obtained several preexisting Id1 transgenic mice from the Benezra lab, MSKCC, and used these to create two mouse strains: (1) a mouse line to study the origin of PDICs using cell-fate tracing experiments and (2) a mouse line to genetically tag PDIC tumor cells to subsequently isolate and culture these cells.

First, we have established a genetic cell-tracking mouse model to specifically and irreversibly label Id1⁺ tumor cells at various time points during tumorigenesis, from premalignant stages through angiogenic switching and tumor establishment.

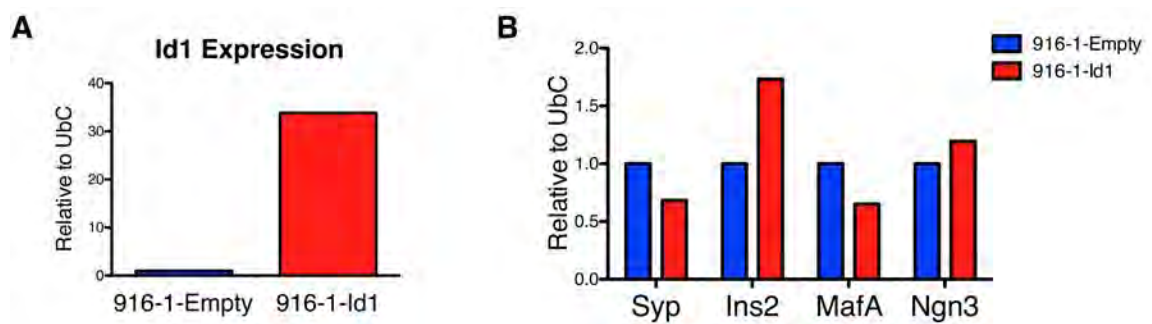


Figure 4.8. Id1 expression in an RT2 tumor cell line. (A) An RT2 tumor cell line (916-1) was infected with either an empty vector or an Id1 expression vector. After several passages the expression of Id1 was examined by qPCR and found to be expressed over 30-fold higher. (B) Expression of β -cell markers synaptophysin (*Syp*), insulin (*Ins2*), *MafA* and Neurogenin3 (*Ngn3*) was examined with qRT-PCR. No differences were seen with the Id1 over-expressing cell line.

Id1^{IRES-creERT2} mice were generated by knocking the bicistronic *Id1-IRES-creERT2* into the endogenous *Id1* locus (Nam and Benezra, 2009). RT2 mice were crossed to *Id1*^{IRES-creERT2} mice and to *Rosa26*^{LSL-LacZ} mice. Thus, *Id1* gene expression drives the expression of a tamoxifen-inducible *Cre* recombinase and upon treatment with tamoxifen, *Cre* removes the premature stop codon preceding LacZ. This irreversibly turns on expression of LacZ to permanently label all cells that express *Id1* at the time of tamoxifen treatment.

We are additionally creating a mouse line in which RT2 mice are crossed to *Id1*^{IRES-creERT2} mice and *Rosa26*^{LSL-YFP} mice. Similar to the strategy described above, upon tamoxifen treatment, all cells that are expressing *Id1* will permanently express YFP. Labeling all *Id1*⁺ PDICs allows isolation using FACS for downstream analysis and genomic profiling. Additionally, PDIC tumor cells will be isolated and cultured to derive PDIC cell lines. These cell lines will be used to study the differences between PDICs and insulinomas. PDIC lines will also be orthotopically injected into the pancreas to create a mouse model of PD-PanNETs that can be used for preclinical testing.

Discussion

Identification of PDICs in RT2 mice

We have described the discovery of a class of tumors, PDICs, that have lost cell differentiation markers, are highly proliferative and anaplastic. Intriguingly, this novel tumor type exhibits many of the characteristics of high grade PD-PanNETs,

a tumor subset of which very little is known and of which patients have very poor prognosis. Studying these tumors may provide important insights into the molecular mechanisms of PD-PanNETs and the use of these tumors to develop a mouse model of PD-PanNETs would be invaluable for use in preclinical testing.

Having serendipitously discovered these tumors through their loss of insulin, we first further characterized these tumors histologically. We found that these tumors had not only lost insulin expression, but were absent for many markers of β -cell differentiation, including those that are expressed in progenitor cells during development. *MafA* is a transcription factor responsible for insulin activation and is expressed only in mature β -cells (Oliver-Krasinski and Stoffers, 2008); thus its absence in RT2 PDICs was consistent with the loss of insulin. Two other transcription factors were found to be absent: *Nkx6.1* and *Pdx1*. *Nkx6.1* is turned on in endocrine progenitors, remains expressed during differentiation and is important for endocrine differentiation (Oliver-Krasinski and Stoffers, 2008). *Pdx1* has been shown to be essential for pancreatic development and β -cell maturation and is expressed in pancreatic progenitors and in immature and mature β -cells (Oliver-Krasinski and Stoffers, 2008). Interestingly, synaptophysin, which is expressed by many cells of the neuroendocrine and neural lineage (Klimstra et al., 2010), maintains at least some expression in PDICs, suggesting that there is still maintenance of some of their neuroendocrine specification.

We also excluded the possibility that these tumors were derived from, or trans-differentiated into, a different cell type by staining for markers of other pancreatic neuroendocrine cells. They did not express markers of alpha-cells or delta-cells, and maintained expression of T-antigen. It is very interesting that tumors that have lost insulin expression still maintain T-antigen expression, as its expression is driven by the rat insulin promoter (RIP), which is controlled in a similar manner to that of the mouse insulin gene. The mechanism of this silencing of insulin expression remains an open question, and one that we hope to address using the mouse models we are developing.

The inhibitor of DNA binding family member Id1 was the first protein that we identified as being specifically expressed in PDICs. Id1 has been shown to be expressed by adult neural stem cells and glioma stem cells (Barrett et al., 2012; Nam and Benezra, 2009). This, combined with the loss of markers of endocrine progenitors, raises the interesting possibility that these tumors may have stem cell-like properties, or perhaps have arisen from a pancreatic stem cell, however this remains to be investigated. To examine if Id1 expression drives PDICs to no longer express insulin by inhibiting their differentiation status, or if it is an indicator of their poorly differentiated state, we overexpressed Id1 in an RT2 tumor cell line. We found that Id1 was not sufficient to induce suppression of β -cell markers, at least in this particular cell line. While this does not exclude the possibility that Id1 overexpression in an *in vivo* tumor setting would change their

differentiation status, it suggests that Id1 is not sufficient to drive these tumors to dedifferentiate.

How do PDICs develop?

Having identified and characterized PDICs histologically, we were very interested in understanding how they develop. We proposed several hypotheses as to how these tumors developed. They could result from a progression from the invasive IC2 class of carcinomas, in which loss of differentiation markers has occurred during the progression to a high-grade tumor. Alternatively, they also could represent a separate tumorigenesis pathway, in which they progress without β -cell markers in a separate pathway to insulinomas. Similarly, they could represent a completely different tumor type, derived from a different cell of origin, whether it be a stem-like cell or another pancreatic neuroendocrine cell.

We have made several very interesting observations that could provide insight into the development of PDICs. The majority of tumors were found to be entirely Id1+, suggesting that tumors arise from a single clone, consistent with the hypothesis that these tumors arise through a separate pathway or cell of origin. However, we found that some tumors exhibited Id1+ cells at the invasive edges of the tumor. This could be indicative of the progression of an invasive tumor cell population that has lost insulin expression. Alternatively, it could again represent a subset of tumor cells that have arisen from a PDIC clone, that is present at the tumor edge. The observation that PDICs exhibit a high mitotic index also brings

into question the timing of their development. With high proliferation rates, it would be expected that PDICs would grow at a much faster rate than insulinomas. However, PDICs are not any larger on average than insulinomas, suggesting that they may arise later than insulinomas. The development of these tumors remains an open question and would provide important insights into the development of PD-PanNETs.

Therefore, we have set up a genetic cell-tracking mouse model (*RT2; Id1^{IRES-creERT2}; Rosa26^{LSL-LacZ}*) to specifically and irreversibly label *Id1*⁺ tumor cells at various time points during tumorigenesis. This cell-tracing system will thus allow us to determine whether PDICs represent: (1) a subsequent stage in PNET progression that develop from insulinomas which have lost markers of differentiation, or (2) instead arise from a completely separate tumorigenic pathway (Figure 4.9). We will treat mice with tamoxifen at the beginning of hyperplasia, at angiogenic switching and then when tumors begin to form to determine when PDICs arise, whether they are *Id1*⁺ from their initiation and whether *Id1* is expressed during any point during the formation of insulinomas.

A previous study has suggested that in the RT2 model, a subset of tumors may arise through a separate pathway (Olson et al., 2009). Through miRNA profiling of a panel of tumors and metastases, they identified a subset of tumors whose gene expression signature clusters closely to that of metastases, and termed these “met-like primary” tumors. They proposed that these met-like primary

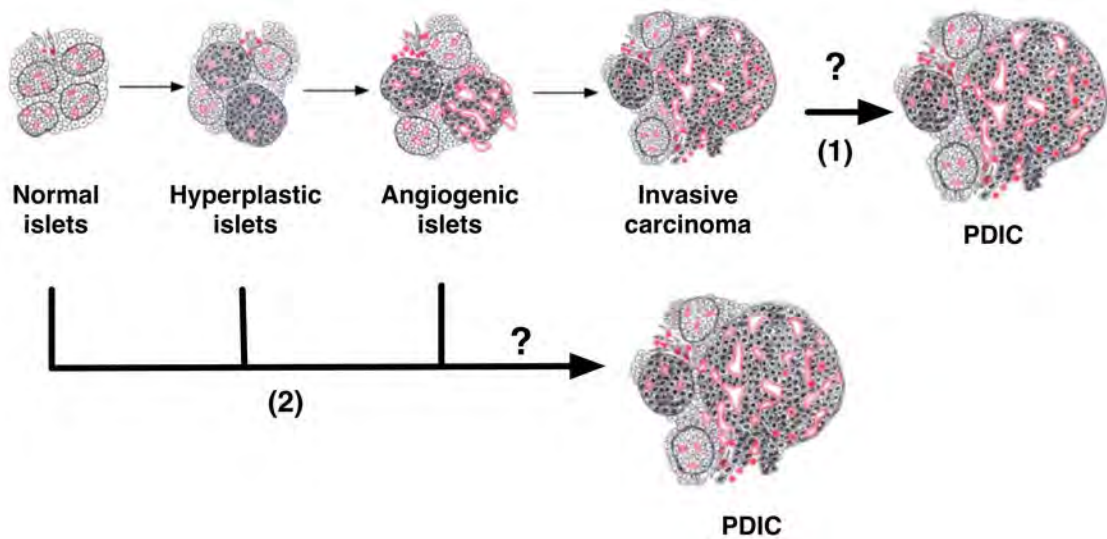


Figure 4.9. PDIC development. PDICs may arise through two distinct pathways: (1) PDICs are a progression from invasive carcinomas that lose expression of β -cell markers or (2) arise through a distinct pathway, potentially from a different cell of origin.

tumors most likely occur through a divergent branch during tumorigenesis, separate from the prototypical progression from encapsulated to invasive classes of tumors. The relatively low frequency of these tumors, making up 10% of the tumors they profiled, and a distinct gene signature from the majority of the tumors, raises the interesting possibility that met-like primary tumors are in fact PDICs. Our cell-fate tracking experiments will provide important insights into the identities of these two tumor types and their developmental pathways.

Development of a mouse model of PD-PanNETs

We have found that PDICs mimic many of the characteristics of PD-PanNETs and have sought to develop a mouse model of PD-PanNETs. To do this, we are creating a mouse strain (RT2; *Id1*^{IRES-creERT2}; *Rosa26*^{LSL-YFP}) in which *Id1*⁺ cells are genetically labeled with YFP, allowing them to be isolated using flow cytometry. We plan to isolate PDIC tumor cells to generate PDIC cell lines. These cell lines will then be orthotopically injected into the pancreata of mice to study these tumors *in vivo* without the complications of the multiple tumors that develop in transgenic RT2 mice. In addition, we can use these isolated cells to profile the molecular characteristics of PDICs. While the results of this study still remain to be determined, we are very excited about its potential, as a PD-PanNET mouse model would be invaluable in screening novel and existing anti-cancer therapeutics.

CHAPTER FIVE

Conclusions, Perspectives and Clinical Implications

Conclusions

Through my thesis research I have aimed to identify tumor cell intrinsic and extrinsic regulators of PanNET pathogenesis using patient samples in combination with the RT2 mouse model of insulinoma. Through the knowledge gained from these studies, we hope to better understand PanNET tumorigenesis, and to develop more effective therapeutics.

Heparanase promotes PanNET tumorigenesis

I first evaluated the role of the matrix remodeling enzyme heparanase in PanNET tumorigenesis. Evaluation of PanNET patient samples revealed that heparanase is significantly correlated with increased tumor stage, advanced tumor grade and metastatic disease in PanNET patients. Additionally, we have shown that heparanase expression is significantly upregulated in the primary tumor and remains high in liver metastases, indicating that elevated heparanase levels observed in the primary tumor may be indicative of metastatic propensity. Heparanase may thus be a useful prognostic indicator for patients that present with PanNETs.

We then sought to understand how heparanase promotes PanNET tumorigenesis by genetically manipulating heparanase levels in the RT2 model of PanNETs. We found that heparanase promotes tumor invasion, through both cancer cell- and macrophage-derived sources. In addition, we found differential effects of heparanase manipulation on angiogenesis and lymphangiogenesis. Heparanase overexpression led to increased peritumoral lymphangiogenesis *in vivo* and enhanced the ability of macrophages to form lymphatic endothelial cell-like structures in culture. Conversely, we found that heparanase deletion led to increased angiogenesis and pericyte coverage.

Characterization and development of a mouse model of PD-PanNETs

We have also identified a subset of RT2 tumors that have lost markers of differentiation that we termed poorly differentiated invasive carcinomas (PDICs). We found that these tumors exhibited a high proliferative index, similar to high-grade PD-PanNETs. Further characterization revealed that PDICs specifically expressed Id1. Using the fact that these tumors specifically express Id1, we are creating mouse models to study the development of PDICs and also to generate PDIC tumor cell lines. These cell lines will then be used to generate an orthotopic implantation model of PD-PanNETs in mice.

Perspectives and Clinical Implications

The multifaceted role of heparanase in tumorigenesis

Through cell based assays and implantation of cancer cell lines, multiple roles for heparanase in promoting tumorigenesis have been previously described (Vlodavsky et al., 2012). Heparanase has been implicated in tumor cell dissemination through its degradation of HSPGs within the ECM (Nakajima et al., 1983; Vlodavsky et al., 1983). Here, we validate this for the first time in a spontaneous mouse model of cancer, finding that heparanase produced by both cancer cells and TAMs significantly promotes tumor invasion. Additionally, we show that this invasion is associated with increased turnover of heparan sulfate at the tumor invasive front, demonstrating the activity of heparanase in HSPG degradation.

Heparanase has also been described to promote growth factor signaling through release of growth factors tethered within the ECM and by the biologically active heparan sulfate fragments. This has been implicated in promoting tumor angiogenesis and lymphangiogenesis (Cohen-Kaplan et al., 2008; Vlodavsky et al., 2012). Interestingly, we see opposing effects in these two processes in RT2 mice. Surprisingly, we saw that while there was no difference in tumor angiogenesis in *Hpa-Tg* RT2 mice, *Hpse*^{-/-} RT2 had increased angiogenesis and pericyte coverage. We hypothesized that this increased angiogenesis was due to the increased heparan sulfate levels found along the blood vessels in *Hpse*^{-/-} RT2 mice, potentially acting as a sink for angiogenic growth factors. While the

increased heparan sulfate levels observed in the *Hpse*^{-/-} RT2 mice are likely due to a lack of heparanase throughout development, it has been described that tumors can exhibit accumulation of HSPGs (Iozzo and Sanderson, 2011). Therefore, it is important to consider the impact of both the cleavage and the accumulation of HSPGs on growth factor signaling.

Increased peritumoral lymphangiogenesis was one of the most striking phenotypes that we identified in the *Hpa*-Tg RT2 mice. In addition, evaluation of head and neck cancer patient samples previously showed a correlation between increased heparanase staining and increased lymphatic density (Cohen-Kaplan et al., 2008), suggesting that heparanase may promote lymphangiogenesis in many tumor types. Evaluation of heparanase overexpression in other mouse model of cancer and in other pathological conditions may provide important insights into the generalizability of this phenotype.

The novel finding that heparanase enhances the ability of macrophages to trans-differentiate into LEC-like structures raises many interesting questions, as the mechanism of how heparanase promotes this process is currently unknown. We identified certain lymphangiogenic growth factors as capable of enhancing this process, however it is unknown whether *Hpa*-Tg macrophages are producing more of these growth factors or have an enhanced response to such factors. In addition, the relevance of this trans-differentiation *in vivo* remains to be determined, however due to technical limitations, we were unable to test this.

Complexities of targeted ECM remodeling enzymes

While previous studies on heparanase have used tumor cell lines, we have utilized a spontaneous model of tumorigenesis to study the activity of heparanase in its endogenous microenvironment for the first time. The importance of investigating matrix-degrading enzymes within the proper microenvironment and appropriate matrix was underscored by our attempts to model tumor invasion in a cell culture system. We were unable to recapitulate the invasion phenotype that we saw *in vivo*, with neither β -tumor cells nor macrophages. While the commonly used matrix Matrigel contains the HSPG perlecan, the composition and the 3D organization of the matrix may not be reflective of that *in vivo*. In addition, HSPGs exert many of their functions through growth factor signaling, which may not be accurately modeled in cell culture systems. Therefore, it is critical to study enzymes such as heparanase in their native *in vivo* microenvironment.

Heparanase as a therapeutic target

Given the previously described roles of heparanase in promoting metastasis and angiogenesis, there has been considerable interest in developing heparanase inhibitors for therapeutic use. Currently, all targeting strategies have used the specificity of heparanase for heparan sulfate to identify heparan sulfate mimetics that inhibit both heparanase activity and block heparan sulfate effector functions,

in particular angiogenesis. In fact, these compounds are described, and typically promoted as anti-angiogenics.

PI-88 (phosphomannopentaose) was the first compound targeting heparanase that was developed. It was identified in a screen of heparan sulfate mimetics for their inhibition of heparanase and for their ability to interfere with heparan sulfate recognition by many angiogenic growth factors (Parish et al., 1999). Preclinical testing showed that it inhibited tumor growth, metastasis and angiogenesis (Joyce et al., 2005; Parish et al., 1999). This compound was further developed and entered into clinical trials. It was found to be generally well tolerated in Phase I trials (Basche et al., 2006) and is currently in a Phase III study for post-resection liver cancer. PI-88 has also been tested in combination with docetaxol in advanced prostate cancer, however this study had to be halted due to hematological toxicity (Khasraw et al., 2010). In addition to PI-88, several other heparan sulfate mimetic compounds have been developed and are entering clinical trials including PG545, SST0001, M402 and DMBO (Basappa et al., 2010; Ferro et al., 2012; Ritchie et al., 2011; Zhou et al., 2011).

The toxicities observed when combining PI-88 with the cytotoxic agent docetaxol, raises the possibility that targeting all heparan sulfate related signaling may lead to increased side effects in the context of cytotoxic therapies, as all heparan sulfate effector functions are inhibited. Therefore, it could be interesting to develop specific inhibitors for heparanase to decrease these side effects.

However, given our results that increased heparan sulfate levels can lead to enhanced growth factor signaling and enhanced angiogenesis, it may be critical to target both heparanase and heparan sulfate mediated signaling at the same time. It is currently unknown what the effects of heparanase and heparan sulfate inhibition are in combination with other therapies. In addition, very few studies have studied the role of heparanase in response to therapy. A recent study showed that increased heparanase expression correlated with response to chemotherapy in laryngeal cancer (Dincer et al., 2012), while another showed that heparanase inhibition can enhance response to radiation therapy (Meirovitz et al., 2011). Therefore, there is great need for preclinical studies on the role of heparanase in response to conventional therapies and to determine whether therapeutic response can be enhanced by simultaneously blocking heparanase functions through combination therapies.

Origin of PDICs

The identification of a subset of RT2 tumors that did not express β -cell markers was very intriguing. These PDICs seem to reflect PD-PanNETs in patients, which also exhibit a high proliferation index and lack of cellular differentiation markers. However, it remains unknown the cell of origin from which both PDICs in mice and PD-PanNETs in humans arise.

Therefore, we are setting up cell-fate tracking experiments to investigate the origin of PDICs. It is unknown whether PDICs arise without markers of β -cell

differentiation, or lose expression of these markers during tumor progression. In addition, it is unknown whether insulinomas ever progress through an Id1⁺ state during their development. PD-PanNETs have been proposed to arise from a progenitor or stem cell within the pancreas (Davies and Conlon, 2009), however this has not been definitively shown. The expression of Id1 by PDICs, which has been shown to be expressed in cancer stem cells (Barrett et al., 2012; O'Brien et al., 2012), raises the interesting possibility that PDICs reflect a stem-like phenotype.

Development of a mouse model of PD-PanNETs

We also plan to use our identification of Id1⁺ PDICs to develop a mouse model of PD-PanNETs. We will isolate PDIC tumor cell lines that will then be orthotopically injected into the pancreata of mice to study these tumors *in vivo*, without the complications of the multiple tumors that develop in transgenic RT2 mice. These tumors will be molecularly profiled and analyzed for the hallmarks of cancer, to gain important insights into PD-PanNET tumorigenesis. We will then validate our results in patient samples, to determine new therapeutic targets for PD-PanNETs. A PD-PanNET mouse model will be invaluable in screening novel and existing anti-cancer therapeutics.

In summary, we have provided novel insights into several tumor cell-intrinsic and tumor cell-extrinsic regulators of PanNET tumorigenesis. We have determined the clinical relevance of heparanase in PanNET tumors and identified it as a

potential prognostic indicator. In addition, we have shown the role of heparanase in promoting invasion and lymphangiogenesis in a PanNET mouse model. Finally, we have identified a novel class of poorly differentiated, highly invasive carcinomas in the mouse model, which are analogous to a poorly understood class of pancreatic cancers in patients. Collectively, my thesis research has opened up multiple new directions in the study of pancreatic neuroendocrine tumors, which may have important clinical implications for the diagnosis, prognosis and future treatment of this disease.

BIBLIOGRAPHY

- Abboud-Jarrous, G., R. Atzmon, T. Peretz, C. Palermo, B.B. Gadea, J.A. Joyce, and I. Vlodavsky. 2008. Cathepsin L is responsible for processing and activation of proheparanase through multiple cleavages of a linker segment. *J Biol Chem.* 283:18167-18176.
- Arvatz, G., I. Shafat, F. Levy-Adam, N. Ilan, and I. Vlodavsky. 2011. The heparanase system and tumor metastasis: is heparanase the seed and soil? *Cancer Metastasis Rev.* 30:253-268.
- Barrett, L.E., Z. Granot, C. Coker, A. Iavarone, D. Hambardzumyan, E.C. Holland, H.S. Nam, and R. Benezra. 2012. Self-renewal does not predict tumor growth potential in mouse models of high-grade glioma. *Cancer Cell.* 21:11-24.
- Basappa, S. Murugan, C.V. Kavitha, A. Purushothaman, K.G. Nevin, K. Sugahara, and K.S. Rangappa. 2010. A small oxazine compound as an anti-tumor agent: a novel pyranoside mimetic that binds to VEGF, HB-EGF, and TNF-alpha. *Cancer Lett.* 297:231-243.
- Basche, M., D.L. Gustafson, S.N. Holden, C.L. O'Bryant, L. Gore, S. Witta, M.K. Schultz, M. Morrow, A. Levin, B.R. Creese, M. Kangas, K. Roberts, T. Nguyen, K. Davis, R.S. Addison, J.C. Moore, and S.G. Eckhardt. 2006. A phase I biological and pharmacologic study of the heparanase inhibitor PI-88 in patients with advanced solid tumors. *Clin Cancer Res.* 12:5471-5480.
- Ben-Zaken, O., I. Shafat, S. Gingis-Velitski, H. Bangio, I.K. Kelson, T. Alergand, Y. Amor, R.B. Maya, I. Vlodavsky, and N. Ilan. 2008. Low and high affinity receptors mediate cellular uptake of heparanase. *Int J Biochem Cell Biol.* 40:530-542.
- Bingle, L., N.J. Brown, and C.E. Lewis. 2002. The role of tumour-associated macrophages in tumour progression: implications for new anticancer therapies. *J Pathol.* 196:254-265.
- Brunner, G., C.N. Metz, H. Nguyen, J. Gabrilove, S.R. Patel, M.A. Davitz, D.B. Rifkin, and E.L. Wilson. 1994. An endogenous glycosylphosphatidylinositol-specific phospholipase D releases basic

fibroblast growth factor-heparan sulfate proteoglycan complexes from human bone marrow cultures. *Blood*. 83:2115-2125.

Chiu, C.W., H. Nozawa, and D. Hanahan. 2010. Survival benefit with proapoptotic molecular and pathologic responses from dual targeting of mammalian target of rapamycin and epidermal growth factor receptor in a preclinical model of pancreatic neuroendocrine carcinogenesis. *J Clin Oncol*. 28:4425-4433.

Cohen-Kaplan, V., I. Naroditsky, A. Zetser, N. Ilan, I. Vlodaysky, and I. Doweck. 2008. Heparanase induces VEGF C and facilitates tumor lymphangiogenesis. *Int J Cancer*. 123:2566-2573.

Davies, K., and K.C. Conlon. 2009. Neuroendocrine tumors of the pancreas. *Curr Gastroenterol Rep*. 11:119-127.

DeNardo, D.G., D.J. Brennan, E. Rexhepaj, B. Ruffell, S.L. Shiao, S.F. Madden, W.M. Gallagher, N. Wadhvani, S.D. Keil, S.A. Junaid, H.S. Rugo, E.S. Hwang, K. Jirstrom, B.L. West, and L.M. Coussens. 2011. Leukocyte complexity predicts breast cancer survival and functionally regulates response to chemotherapy. *Cancer Discov*. 1:54-67.

Dincer, M., K. Altundag, M. Cengiz, E. Ozyar, A. Sungur, S. Hosal, and I.H. Gullu. 2012. Tumor heparanase expression in predicting response to induction chemotherapy in patients with locally advanced laryngeal cancer. *J BUON*. 17:337-342.

Edge, S.B., and C.C. Compton. 2010. The American Joint Committee on Cancer: the 7th edition of the AJCC cancer staging manual and the future of TNM. *Ann Surg Oncol*. 17:1471-1474.

Ferro, V., L. Liu, K.D. Johnstone, N. Wimmer, T. Karoli, P. Handley, J. Rowley, K. Dredge, C.P. Li, E. Hammond, K. Davis, L. Sarimaa, J. Harenberg, and I. Bytheway. 2012. Discovery of PG545: a highly potent and simultaneous inhibitor of angiogenesis, tumor growth, and metastasis. *J Med Chem*. 55:3804-3813.

Ferrone, C.R., L.H. Tang, J. Tomlinson, M. Gonen, S.N. Hochwald, M.F. Brennan, D.S. Klimstra, and P.J. Allen. 2007. Determining prognosis in patients with pancreatic endocrine neoplasms: can the WHO classification system be simplified? *J Clin Oncol*. 25:5609-5615.

- Folkman, J. 1971. Tumor angiogenesis: therapeutic implications. *N Engl J Med.* 285:1182-1186.
- Folkman, J., K. Watson, D. Ingber, and D. Hanahan. 1989. Induction of angiogenesis during the transition from hyperplasia to neoplasia. *Nature.* 339:58-61.
- Fux, L., N. Ilan, R.D. Sanderson, and I. Vlodavsky. 2009. Heparanase: busy at the cell surface. *Trends Biochem Sci.* 34:511-519.
- Gocheva, V., H.W. Wang, B.B. Gadea, T. Shree, K.E. Hunter, A.L. Garfall, T. Berman, and J.A. Joyce. 2010. IL-4 induces cathepsin protease activity in tumor-associated macrophages to promote cancer growth and invasion. *Genes Dev.* 24:241-255.
- Halfdanarson, T.R., J. Rubin, M.B. Farnell, C.S. Grant, and G.M. Petersen. 2008. Pancreatic endocrine neoplasms: epidemiology and prognosis of pancreatic endocrine tumors. *Endocr Relat Cancer.* 15:409-427.
- Hanahan, D. 1985. Heritable formation of pancreatic beta-cell tumours in transgenic mice expressing recombinant insulin/simian virus 40 oncogenes. *Nature.* 315:115-122.
- He, Y., I. Rajantie, M. Ilmonen, T. Makinen, M.J. Karkkainen, P. Haiko, P. Salven, and K. Alitalo. 2004. Preexisting lymphatic endothelium but not endothelial progenitor cells are essential for tumor lymphangiogenesis and lymphatic metastasis. *Cancer Res.* 64:3737-3740.
- Hermano, E., I. Lerner, and M. Elkin. 2012. Heparanase enzyme in chronic inflammatory bowel disease and colon cancer. *Cell Mol Life Sci.* 69:2501-2513.
- Hu, W., Z. Feng, I. Modica, D.S. Klimstra, L. Song, P.J. Allen, M.F. Brennan, A.J. Levine, and L.H. Tang. 2010. Gene Amplifications in Well-Differentiated Pancreatic Neuroendocrine Tumors Inactivate the p53 Pathway. *Genes Cancer.* 1:360-368.
- Hulett, M.D., C. Freeman, B.J. Hamdorf, R.T. Baker, M.J. Harris, and C.R. Parish. 1999. Cloning of mammalian heparanase, an important enzyme in tumor invasion and metastasis. *Nat Med.* 5:803-809.

- Hulett, M.D., J.R. Hornby, S.J. Ohms, J. Zuegg, C. Freeman, J.E. Gready, and C.R. Parish. 2000. Identification of active-site residues of the pro-metastatic endoglycosidase heparanase. *Biochemistry*. 39:15659-15667.
- Iozzo, R.V., and R.D. Sanderson. 2011. Proteoglycans in cancer biology, tumour microenvironment and angiogenesis. *J Cell Mol Med*. 15:1013-1031.
- Jiang, S., A.S. Bailey, D.C. Goldman, J.R. Swain, M.H. Wong, P.R. Streeter, and W.H. Fleming. 2008. Hematopoietic stem cells contribute to lymphatic endothelium. *PLoS One*. 3:e3812.
- Jiao, Y., C. Shi, B.H. Edil, R.F. de Wilde, D.S. Klimstra, A. Maitra, R.D. Schulick, L.H. Tang, C.L. Wolfgang, M.A. Choti, V.E. Velculescu, L.A. Diaz, Jr., B. Vogelstein, K.W. Kinzler, R.H. Hruban, and N. Papadopoulos. 2011. DAXX/ATRX, MEN1, and mTOR pathway genes are frequently altered in pancreatic neuroendocrine tumors. *Science*. 331:1199-1203.
- Joyce, J.A., C. Freeman, N. Meyer-Morse, C.R. Parish, and D. Hanahan. 2005. A functional heparan sulfate mimetic implicates both heparanase and heparan sulfate in tumor angiogenesis and invasion in a mouse model of multistage cancer. *Oncogene*. 24:4037-4051.
- Joyce, J.A., and J.W. Pollard. 2009. Microenvironmental regulation of metastasis. *Nat Rev Cancer*. 9:239-252.
- Kerjaschki, D., N. Huttary, I. Raab, H. Regele, K. Bojarski-Nagy, G. Bartel, S.M. Krober, H. Greinix, A. Rosenmaier, F. Karlhofer, N. Wick, and P.R. Mazal. 2006. Lymphatic endothelial progenitor cells contribute to de novo lymphangiogenesis in human renal transplants. *Nat Med*. 12:230-234.
- Khasraw, M., N. Pavlakis, S. McCowatt, C. Underhill, S. Begbie, P. de Souza, A. Boyce, F. Parnis, V. Lim, R. Harvie, and G. Marx. 2010. Multicentre phase I/II study of PI-88, a heparanase inhibitor in combination with docetaxel in patients with metastatic castrate-resistant prostate cancer. *Ann Oncol*. 21:1302-1307.
- Kim, S.H., J. Turnbull, and S. Guimond. 2011. Extracellular matrix and cell signalling: the dynamic cooperation of integrin, proteoglycan and growth factor receptor. *J Endocrinol*. 209:139-151.

- Klimstra, D.S., I.R. Modlin, D. Coppola, R.V. Lloyd, and S. Suster. 2010. The pathologic classification of neuroendocrine tumors: a review of nomenclature, grading, and staging systems. *Pancreas*. 39:707-712.
- Kulke, M.H., J. Bendell, L. Kvols, J. Picus, R. Pommier, and J. Yao. 2011. Evolving diagnostic and treatment strategies for pancreatic neuroendocrine tumors. *J Hematol Oncol*. 4:29.
- Kussie, P.H., J.D. Hulmes, D.L. Ludwig, S. Patel, E.C. Navarro, A.P. Seddon, N.A. Giorgio, and P. Bohlen. 1999. Cloning and functional expression of a human heparanase gene. *Biochem Biophys Res Commun*. 261:183-187.
- Lerner, I., E. Hermano, E. Zcharia, D. Rodkin, R. Bulvik, V. Doviner, A.M. Rubinstein, R. Ishai-Michaeli, R. Atzmon, Y. Sherman, A. Meirovitz, T. Peretz, I. Vlodaysky, and M. Elkin. 2011. Heparanase powers a chronic inflammatory circuit that promotes colitis-associated tumorigenesis in mice. *J Clin Invest*. 121:1709-1721.
- Levy-Adam, F., S. Feld, V. Cohen-Kaplan, A. Shteingauz, M. Gross, G. Arvatz, I. Naroditsky, N. Ilan, I. Doweck, and I. Vlodaysky. 2010. Heparanase 2 interacts with heparan sulfate with high affinity and inhibits heparanase activity. *J Biol Chem*. 285:28010-28019.
- Levy-Adam, F., H.Q. Miao, R.L. Henrikson, I. Vlodaysky, and N. Ilan. 2003. Heterodimer formation is essential for heparanase enzymatic activity. *Biochem Biophys Res Commun*. 308:885-891.
- Lewis, C.E., and J.W. Pollard. 2006. Distinct role of macrophages in different tumor microenvironments. *Cancer Res*. 66:605-612.
- Lopez, T., and D. Hanahan. 2002. Elevated levels of IGF-1 receptor convey invasive and metastatic capability in a mouse model of pancreatic islet tumorigenesis. *Cancer Cell*. 1:339-353.
- Lyden, D., A.Z. Young, D. Zagzag, W. Yan, W. Gerald, R. O'Reilly, B.L. Bader, R.O. Hynes, Y. Zhuang, K. Manova, and R. Benezra. 1999. Id1 and Id3 are required for neurogenesis, angiogenesis and vascularization of tumour xenografts. *Nature*. 401:670-677.

- Mandriota, S.J., L. Jussila, M. Jeltsch, A. Compagni, D. Baetens, R. Prevo, S. Banerji, J. Huarte, R. Montesano, D.G. Jackson, L. Orci, K. Alitalo, G. Christofori, and M.S. Pepper. 2001. Vascular endothelial growth factor-C-mediated lymphangiogenesis promotes tumour metastasis. *EMBO J.* 20:672-682.
- Manon-Jensen, T., Y. Itoh, and J.R. Couchman. 2010. Proteoglycans in health and disease: the multiple roles of syndecan shedding. *FEBS J.* 277:3876-3889.
- Mantovani, A., P. Allavena, A. Sica, and F. Balkwill. 2008. Cancer-related inflammation. *Nature.* 454:436-444.
- Maruyama, K., M. Ii, C. Cursiefen, D.G. Jackson, H. Keino, M. Tomita, N. Van Rooijen, H. Takenaka, P.A. D'Amore, J. Stein-Streilein, D.W. Losordo, and J.W. Streilein. 2005. Inflammation-induced lymphangiogenesis in the cornea arises from CD11b-positive macrophages. *J Clin Invest.* 115:2363-2372.
- Mccullagh, P. 1980. Regression-Models for Ordinal Data. *Journal of the Royal Statistical Society Series B-Methodological.* 42:109-142.
- McKenzie, E., K. Tyson, A. Stamps, P. Smith, P. Turner, R. Barry, M. Hircock, S. Patel, E. Barry, C. Stubberfield, J. Terrett, and M. Page. 2000. Cloning and expression profiling of Hpa2, a novel mammalian heparanase family member. *Biochem Biophys Res Commun.* 276:1170-1177.
- Meirovitz, A., E. Hermano, I. Lerner, E. Zcharia, C. Pisano, T. Peretz, and M. Elkin. 2011. Role of heparanase in radiation-enhanced invasiveness of pancreatic carcinoma. *Cancer Res.* 71:2772-2780.
- Moertel, C.G., L.K. Kvols, M.J. O'Connell, and J. Rubin. 1991. Treatment of neuroendocrine carcinomas with combined etoposide and cisplatin. Evidence of major therapeutic activity in the anaplastic variants of these neoplasms. *Cancer.* 68:227-232.
- Nakajima, M., T. Irimura, D. Di Ferrante, N. Di Ferrante, and G.L. Nicolson. 1983. Heparan sulfate degradation: relation to tumor invasive and metastatic properties of mouse B16 melanoma sublines. *Science.* 220:611-613.

- Nam, H.S., and R. Benezra. 2009. High levels of Id1 expression define B1 type adult neural stem cells. *Cell Stem Cell*. 5:515-526.
- Nolan-Stevaux, O., M.C. Truitt, J.C. Pahler, P. Olson, C. Guinto, D.C. Lee, and D. Hanahan. 2010. Differential contribution to neuroendocrine tumorigenesis of parallel egfr signaling in cancer cells and pericytes. *Genes Cancer*. 1:125-141.
- O'Brien, C.A., A. Kreso, P. Ryan, K.G. Hermans, L. Gibson, Y. Wang, A. Tsatsanis, S. Gallinger, and J.E. Dick. 2012. ID1 and ID3 regulate the self-renewal capacity of human colon cancer-initiating cells through p21. *Cancer Cell*. 21:777-792.
- Okabe, M., M. Ikawa, K. Kominami, T. Nakanishi, and Y. Nishimune. 1997. 'Green mice' as a source of ubiquitous green cells. *FEBS Lett*. 407:313-319.
- Oliver-Krasinski, J.M., and D.A. Stoffers. 2008. On the origin of the beta cell. *Genes Dev*. 22:1998-2021.
- Olson, P., J. Lu, H. Zhang, A. Shai, M.G. Chun, Y. Wang, S.K. Libutti, E.K. Nakakura, T.R. Golub, and D. Hanahan. 2009. MicroRNA dynamics in the stages of tumorigenesis correlate with hallmark capabilities of cancer. *Genes Dev*. 23:2152-2165.
- Paez-Ribes, M., E. Allen, J. Hudock, T. Takeda, H. Okuyama, F. Vinals, M. Inoue, G. Bergers, D. Hanahan, and O. Casanovas. 2009. Antiangiogenic therapy elicits malignant progression of tumors to increased local invasion and distant metastasis. *Cancer Cell*. 15:220-231.
- Paget, S. 1989. The distribution of secondary growths in cancer of the breast. 1889. *Cancer Metastasis Rev*. 8:98-101.
- Parish, C.R., C. Freeman, K.J. Brown, D.J. Francis, and W.B. Cowden. 1999. Identification of sulfated oligosaccharide-based inhibitors of tumor growth and metastasis using novel in vitro assays for angiogenesis and heparanase activity. *Cancer Res*. 59:3433-3441.
- Perk, J., A. Iavarone, and R. Benezra. 2005. Id family of helix-loop-helix proteins in cancer. *Nat Rev Cancer*. 5:603-614.

- Pyonteck, S.M., B.B. Gadea, H.W. Wang, V. Gocheva, K.E. Hunter, L.H. Tang, and J.A. Joyce. 2012. Deficiency of the macrophage growth factor CSF-1 disrupts pancreatic neuroendocrine tumor development. *Oncogene*. 31:1459-1467.
- Raymond, E., L. Dahan, J.L. Raoul, Y.J. Bang, I. Borbath, C. Lombard-Bohas, J. Valle, P. Metrakos, D. Smith, A. Vinik, J.S. Chen, D. Horsch, P. Hammel, B. Wiedenmann, E. Van Cutsem, S. Patyna, D.R. Lu, C. Blanckmeister, R. Chao, and P. Ruzzniewski. 2011. Sunitinib malate for the treatment of pancreatic neuroendocrine tumors. *N Engl J Med*. 364:501-513.
- Reidy, D.L., L.H. Tang, and L.B. Saltz. 2009. Treatment of advanced disease in patients with well-differentiated neuroendocrine tumors. *Nat Clin Pract Oncol*. 6:143-152.
- Reidy-Lagunes, D.L. 2012. Systemic therapy for advanced pancreatic neuroendocrine tumors: an update. *J Natl Compr Canc Netw*. 10:777-783.
- Religa, P., R. Cao, M. Bjorndahl, Z. Zhou, Z. Zhu, and Y. Cao. 2005. Presence of bone marrow-derived circulating progenitor endothelial cells in the newly formed lymphatic vessels. *Blood*. 106:4184-4190.
- Ribatti, D., B. Nico, E. Crivellato, A.M. Roccaro, and A. Vacca. 2007. The history of the angiogenic switch concept. *Leukemia*. 21:44-52.
- Ritchie, J.P., V.C. Ramani, Y. Ren, A. Naggi, G. Torri, B. Casu, S. Penco, C. Pisano, P. Carminati, M. Tortoreto, F. Zunino, I. Vlodavsky, R.D. Sanderson, and Y. Yang. 2011. SST0001, a chemically modified heparin, inhibits myeloma growth and angiogenesis via disruption of the heparanase/syndecan-1 axis. *Clin Cancer Res*. 17:1382-1393.
- Shree, T., O.C. Olson, B.T. Elie, J.C. Kester, A.L. Garfall, K. Simpson, K.M. Bell-McGuinn, E.C. Zabor, E. Brogi, and J.A. Joyce. 2011. Macrophages and cathepsin proteases blunt chemotherapeutic response in breast cancer. *Genes Dev*. 25:2465-2479.
- Siegel, R., D. Naishadham, and A. Jemal. 2012. Cancer statistics, 2012. *CA Cancer J Clin*. 62:10-29.

- Skobe, M., T. Hawighorst, D.G. Jackson, R. Prevo, L. Janes, P. Velasco, L. Riccardi, K. Alitalo, K. Claffey, and M. Detmar. 2001. Induction of tumor lymphangiogenesis by VEGF-C promotes breast cancer metastasis. *Nat Med.* 7:192-198.
- Soriano, P. 1999. Generalized lacZ expression with the ROSA26 Cre reporter strain. *Nat Genet.* 21:70-71.
- Srinivas, S., T. Watanabe, C.S. Lin, C.M. Williams, Y. Tanabe, T.M. Jessell, and F. Costantini. 2001. Cre reporter strains produced by targeted insertion of EYFP and ECFP into the ROSA26 locus. *BMC Dev Biol.* 1:4.
- Sundar, S.S., and T.S. Ganesan. 2007. Role of lymphangiogenesis in cancer. *J Clin Oncol.* 25:4298-4307.
- Tammela, T., and K. Alitalo. 2010. Lymphangiogenesis: Molecular mechanisms and future promise. *Cell.* 140:460-476.
- Thorel, F., V. Nepote, I. Avril, K. Kohno, R. Desgraz, S. Chera, and P.L. Herrera. 2010. Conversion of adult pancreatic alpha-cells to beta-cells after extreme beta-cell loss. *Nature.* 464:1149-1154.
- Toyoshima, M., and M. Nakajima. 1999. Human heparanase. Purification, characterization, cloning, and expression. *J Biol Chem.* 274:24153-24160.
- Tuveson, D., and D. Hanahan. 2011. Translational medicine: Cancer lessons from mice to humans. *Nature.* 471:316-317.
- Vlodavsky, I., P. Beckhove, I. Lerner, C. Pisano, A. Meirovitz, N. Ilan, and M. Elkin. 2012. Significance of heparanase in cancer and inflammation. *Cancer Microenviron.* 5:115-132.
- Vlodavsky, I., Y. Friedmann, M. Elkin, H. Aingorn, R. Atzmon, R. Ishai-Michaeli, M. Bitan, O. Pappo, T. Peretz, I. Michal, L. Spector, and I. Pecker. 1999. Mammalian heparanase: gene cloning, expression and function in tumor progression and metastasis. *Nat Med.* 5:793-802.
- Vlodavsky, I., Z. Fuks, M. Bar-Ner, Y. Ariav, and V. Schirrmacher. 1983. Lymphoma cell-mediated degradation of sulfated proteoglycans in the

subendothelial extracellular matrix: relationship to tumor cell metastasis. *Cancer Res.* 43:2704-2711.

Vogelzang, N.J., S.I. Benowitz, S. Adams, C. Aghajanian, S.M. Chang, Z.E. Dreyer, P.A. Janne, A.H. Ko, G.A. Masters, O. Odenike, J.D. Patel, B.J. Roth, W.E. Samlowski, A.D. Seidman, W.D. Tap, J.S. Temel, J.H. Von Roenn, and M.G. Kris. 2012. Clinical cancer advances 2011: Annual Report on Progress Against Cancer from the American Society of Clinical Oncology. *J Clin Oncol.* 30:88-109.

Yao, J.C., M.P. Eisner, C. Leary, C. Dagohoy, A. Phan, A. Rashid, M. Hassan, and D.B. Evans. 2007. Population-based study of islet cell carcinoma. *Ann Surg Oncol.* 14:3492-3500.

Yao, J.C., M. Hassan, A. Phan, C. Dagohoy, C. Leary, J.E. Mares, E.K. Abdalla, J.B. Fleming, J.N. Vauthey, A. Rashid, and D.B. Evans. 2008. One hundred years after "carcinoid": epidemiology of and prognostic factors for neuroendocrine tumors in 35,825 cases in the United States. *J Clin Oncol.* 26:3063-3072.

Yao, J.C., M.H. Shah, T. Ito, C.L. Bohas, E.M. Wolin, E. Van Cutsem, T.J. Hobday, T. Okusaka, J. Capdevila, E.G. de Vries, P. Tomassetti, M.E. Pavel, S. Hoosen, T. Haas, J. Lincy, D. Lebwohl, and K. Oberg. 2011. Everolimus for advanced pancreatic neuroendocrine tumors. *N Engl J Med.* 364:514-523.

Zcharia, E., J. Jia, X. Zhang, L. Baraz, U. Lindahl, T. Peretz, I. Vlodavsky, and J.P. Li. 2009. Newly generated heparanase knock-out mice unravel co-regulation of heparanase and matrix metalloproteinases. *PLoS One.* 4:e5181.

Zcharia, E., S. Metzger, T. Chajek-Shaul, H. Aingorn, M. Elkin, Y. Friedmann, T. Weinstein, J.P. Li, U. Lindahl, and I. Vlodavsky. 2004. Transgenic expression of mammalian heparanase uncovers physiological functions of heparan sulfate in tissue morphogenesis, vascularization, and feeding behavior. *FASEB J.* 18:252-263.

Zcharia, E., R. Zilka, A. Yaar, O. Yacoby-Zeevi, A. Zetser, S. Metzger, R. Sarid, A. Naggi, B. Casu, N. Ilan, I. Vlodavsky, and R. Abramovitch. 2005. Heparanase accelerates wound angiogenesis and wound healing in mouse and rat models. *FASEB J.* 19:211-221.

Zhou, H., S. Roy, E. Cochran, R. Zouaoui, C.L. Chu, J. Duffner, G. Zhao, S. Smith, Z. Galcheva-Gargova, J. Karlgren, N. Dussault, R.Y. Kwan, E. Moy, M. Barnes, A. Long, C. Honan, Y.W. Qi, Z. Shriver, T. Ganguly, B. Schultes, G. Venkataraman, and T.K. Kishimoto. 2011. M402, a novel heparan sulfate mimetic, targets multiple pathways implicated in tumor progression and metastasis. *PLoS One*. 6:e21106.

Zumsteg, A., V. Baeriswyl, N. Imaizumi, R. Schwendener, C. Ruegg, and G. Christofori. 2009. Myeloid cells contribute to tumor lymphangiogenesis. *PLoS One*. 4:e7067.

Zumsteg, A., and G. Christofori. 2012. Myeloid cells and lymphangiogenesis. *Cold Spring Harb Perspect Med*. 2:a006494.